



HAL
open science

A Three-player Nash game for point-wise source identification in Cauchy-Stokes problems

Marwa Ouni, Abderrahmane Habbal, Moez Kallel

► **To cite this version:**

Marwa Ouni, Abderrahmane Habbal, Moez Kallel. A Three-player Nash game for point-wise source identification in Cauchy-Stokes problems. 2022. hal-03523088v1

HAL Id: hal-03523088

<https://inria.hal.science/hal-03523088v1>

Preprint submitted on 13 Jan 2022 (v1), last revised 13 Jan 2023 (v2)

HAL is a multi-disciplinary open access archive for the deposit and dissemination of scientific research documents, whether they are published or not. The documents may come from teaching and research institutions in France or abroad, or from public or private research centers.

L'archive ouverte pluridisciplinaire **HAL**, est destinée au dépôt et à la diffusion de documents scientifiques de niveau recherche, publiés ou non, émanant des établissements d'enseignement et de recherche français ou étrangers, des laboratoires publics ou privés.

A Three-player Nash game for point-wise source identification in Cauchy-Stokes problems

Marwa OUNI^{a,c,*}, Abderrahmane HABBAL^{a,b}, Moez KALLEL^c

^aUniversity of Côte d'Azur, LJAD, Parc Valrose 06108 Nice, France

^bPolytechnic Mohammed VI University, Benguerir, Morocco

^cUniversity of Tunis El Manar, ENIT-LAMSIN, BP 37, 1002 Tunis-Belvédère, Tunisia

Abstract

We consider linear steady Stokes flow under the action of a finite number of particles located inside the flow domain. The particles exert point-wise forces on the fluid, and are unknown in number, location and magnitude. We are interested in the determination of these point-wise forces, using only a single pair of partially available Cauchy boundary measurements. The inverse problem then couples two harsh problems : identification of point-wise sources and recovery of missing boundary data. We reformulate it as a three-player Nash game. The first two players aim at recovering the Dirichlet and Neumann missing data, while the third one aims at the point-forces reconstruction of the number, location and magnitude of the point-forces. To illustrate the efficiency and robustness of the proposed algorithm, we finally present several numerical experiments for different geometries and source distribution, including the case of noisy measurements.

Keywords: Data completion, Point-force detection, Topological sensitivity, Nash game

1. Introduction

Consider a bounded open domain $\Omega \subset \mathbb{R}^d$ ($d=2, 3$) occupied by an incompressible viscous fluid, with a smooth enough boundary $\partial\Omega$. We assume that the fluid flow is under the action of a finite number of point-wise forces F located inside Ω .

The source term F is assumed to be a linear combination of Dirac distributions accounting for the collection of the point-wise forces:

$$F = \sum_{k=1}^m \lambda_k \delta_{P_k}, \quad (1)$$

where m is the total number of point-wise forces, δ_{P_k} denotes the classical Dirac distribution with origin the point P_k , and $\lambda_k \in \mathbb{R}^d$ is a constant vector. The parameters P_k and λ_k stand respectively for the position and the magnitude of the k th point-wise force.

In this work, we assume that the vectors λ_k are nonzero and that the positions P_k are well separated and satisfy the following :

$$\begin{aligned} P_k \neq P_{k'}, \quad \forall k \neq k' \text{ and } \lambda_k \neq 0 \quad \forall k, k' \in \{1, \dots, m\}, \\ \text{dist}(P_k, \partial\Omega) \geq d_0 > 0, \quad \forall k \in \{1, \dots, m\}. \end{aligned} \quad (2)$$

The Cauchy-Stokes inverse problem consists then in a coupled inverse problem : identification of point-wise sources, and recovery of missing boundary data.

*Corresponding author

Email addresses: marwa1ouni@gmail.com (Marwa OUNI), habbal@unice.fr (Abderrahmane HABBAL), moez.kallel@enit.utm.tn (Moez KALLEL)

1 The first inverse problem is a classical point-wise source reconstruction. Namely, from given velocity G
 2 and fluid stress forces Φ prescribed on Γ_c , where Γ_c is a part of the boundary $\partial\Omega$, one has to identify the
 3 unknown source-term F^* , that is, to find the number, the location and the magnitude of these point-wise
 4 forces such that the fluid velocity u and the pressure p are solution of the following Stokes problem:

$$(\mathcal{CS}) \begin{cases} -\operatorname{div}(\sigma(u, p)) = F^* & \text{in } \Omega, \\ \operatorname{div} u = 0 & \text{in } \Omega, \\ u = G & \text{on } \Gamma_c, \\ \sigma(u, p)n = \Phi & \text{on } \Gamma_c, \end{cases}$$

where n is the unit outward normal vector on the boundary, and $\sigma(u, p)$ the fluid stress tensor defined as follows:

$$\sigma(u, p) = -pI_d + 2\nu D(u)$$

5 with $D(u) = \frac{1}{2}(\nabla u + \nabla u^T)$ being the linear strain tensor, I_d denotes the $d \times d$ identity matrix and $\nu > 0$ is
 6 a viscosity coefficient that remains constant for all values of applied shear stress. For simplicity and without
 7 loss of generality, from now on, the viscosity to be equal unity.

8
 9 Additionally to the inverse problem of detecting the unknown point-wise sources, one has to complete
 10 the boundary data, that is to recover the missing traces of the velocity u and of the normal stress $\sigma(u, p)n$
 11 over $\bar{\Gamma}_i$, the inaccessible part of the boundary. This inverse problem is of Cauchy type, a family of problems
 12 known to be severely ill-posed in the sense of Hadamard [17], even regardless of the point-wise force identi-
 13 fication, because the existence of solution is not guaranteed for arbitrary Cauchy data and depends on their
 14 *compatibility*, and even if a solution exists, it is unstable with respect to small perturbations of the Cauchy
 15 data.

16
 17 For the Cauchy problem, there exists a prolific dedicated literature. An excerpt of popular approaches
 18 are the least-square penalty techniques, as used in [12] and in the earlier paper [14], Tikhonov regularization
 19 methods [7], quasi reversibility methods [4], alternating iterative methods [20, 19] and control type methods
 20 [24, 1]. Recently, an approach based on game theory, using decentralized strategies, was proposed in [15].
 21 The same approach has been investigated in [6] for the solution of coupled conductivity identification and
 22 data completion in cardiac electrophysiology, and in [16] to solve the problem of detecting unknown cavities
 23 immersed in a stationary viscous fluid using partial boundary measurements.

24
 25 The point-wise force identification for the Stokes system was, in contrast, paid much less attention.
 26 The authors in [2] introduced an approach based on considering a reciprocity gap functional for *Stokeslets*
 27 located outside Ω . In [13], the authors proposed to detect the point-force locations by minimizing tracking
 28 (a difference to a distributed state known all over Ω) and energy functionals. Their algorithm is based on
 29 a relaxation technique and on topological sensitivity analysis. We shall follow the same lines for the source
 30 identification algorithmic part of our coupled inverse problem. To the best of our knowledge, there are
 31 no papers which address algorithmic aspects in solving the present coupled point-wise source identification
 32 and boundary data recovery problems for the steady Stokes flows. The paper [21] addresses the coupled
 33 inverse problem of identifying wells and recovering boundary data, but with the help of a number of interior
 34 measurements. We can also mention an earlier paper made by El Badia and Ha-Duong [9] for an inverse
 35 source problem for elliptic equations. Its application aims to identify electrostatic dipoles in the human
 36 head where the boundary data are generated via electrodes placed on the head's part. The authors give a
 37 uniqueness result and an algebraic method for computing the number of dipoles and their characteristics.

38
 39 The paper is organized as follows. In section 2, we introduce the identifiability problem for the Cauchy-
 40 Stokes case, and we provide an identifiability result. Then, using a relaxed formulation in section 3, we
 41 formulate a Nash game approach to tackle the coupled problem of detecting the unknown point-forces and
 42 recovering the missing boundary data. A topological sensitivity analysis method is used in order to determine
 43 the optimal location of the point-sources. We present what we think is a fairly new algorithm. Optimization

1 (sub)tasks are performed by means of descend methods, so *ad hoc* adjoint state methods are provided to
 2 compute the gradients.

3 Finally, Section 4 illustrates the efficiency and robustness of the proposed overall method, where different
 4 numerical experiments are presented and discussed. We end paper by a short concluding section.

5
 6 **Some notation:** Let Ω be a bounded domain in \mathbb{R}^d ($d=2$ or 3), with Lipschitz boundary $\partial\Omega$. Let Γ_c be
 7 an open part of $\partial\Omega$ and we put $\Gamma_i = \partial\Omega \setminus \Gamma_c$. For any subset $\Gamma = \Gamma_c$ or Γ_i , the space of function in $H^1(\Omega)^d$
 8 vanishing on Γ is denoted by $H_\Gamma^1(\Omega)$. By $H^{\frac{1}{2}}(\Gamma)^d$, we denote the space of traces of functions of $H^1(\Omega)^d$ over
 9 Γ . Furthermore, we will use the special space $H_{00}^{\frac{1}{2}}(\Gamma)^d$, which consists of functions from $H^{\frac{1}{2}}(\Gamma)^d$ vanishing
 10 on $\partial\Omega \setminus \Gamma$. This is a subspace of $H^{\frac{1}{2}}(\Gamma)^d$ and its dual space is then denoted by $(H_{00}^{\frac{1}{2}}(\Gamma)^d)'$.

11 2. An identifiability result for the inverse point-forces Cauchy-Stokes problem

12 The source identifiability problem amounts to ask whether a unique pair of over specified boundary data,
 13 for instance the Cauchy data (G, Φ) , could reconstruct a unique source, and if not, how much of such pairs
 14 is necessary to a unique reconstruction.

15 Our identifiability result is given by the following theorem:

16 **Theorem 1.** *Let be $\Omega \subset \mathbb{R}^d$ an open bounded Lipschitz domain and Γ_c a non-empty open subset of the*
 17 *boundary $\partial\Omega$. Consider two point-wise source terms F_1 and F_2 of the form (1), whose magnitudes and*
 18 *locations satisfy the requirements stated in (2).*

For $i = 1, 2$, let be (u_i, p_i) the solution of the following :

$$\begin{cases} -\operatorname{div}(\sigma(u_i, p_i)) = F_i & \text{in } \Omega, \\ \operatorname{div} u_i = 0 & \text{in } \Omega, \\ u_i = G & \text{on } \Gamma_c, \\ \sigma(u_i, p_i)n = \Phi & \text{on } \Gamma_c. \end{cases} \quad (3)$$

where the Cauchy data $(G, \Phi) \in H^{\frac{1}{2}}(\Gamma_c)^d \times (H_{00}^{\frac{1}{2}}(\Gamma_c)^d)'$ are assumed to be compatible for the two Cauchy-Stokes problems. Then $F_1 = F_2$, that is,

$$m_1 = m_2 = m, \quad \{(\lambda_{k,1}, P_{k,1}), 1 \leq k \leq m\} = \{(\lambda_{k',2}, P_{k',2}), 1 \leq k' \leq m\}.$$

19 *Proof:* An identifiability result is proved for the Dirac-Stokes problem in [2] using the reciprocity gap.
 20 In our general framework, proofs of identifiability usually follow the same classical steps by properly using
 21 the unique continuation property, notably for second order elliptic PDES. We follow the same lines, with
 22 slight adaption to our Cauchy-Stokes problem.

23 Let (u_i, p_i) , $i=1,2$ be solutions to the system (3), and we define $(v, q) = (u_1 - u_2, p_1 - p_2)$ and $F = F_1 - F_2$, where

$$F = \sum_{k=1}^{m_1} \lambda_{k,1} \delta_{P_{k,1}} - \sum_{k'=1}^{m_2} \lambda_{k',2} \delta_{P_{k',2}}, \quad \forall k, k' = 1, \dots, m_i \text{ and } i = 1, 2.$$

It is straightforward to see that (v, q) is a solution of

$$(\mathcal{P}) \begin{cases} -\operatorname{div}(\sigma(v, q)) = F & \text{in } \Omega, \\ \operatorname{div} v = 0 & \text{in } \Omega, \\ v = 0 & \text{on } \Gamma_c, \\ \sigma(v, q)n = 0 & \text{on } \Gamma_c. \end{cases}$$

Consider $(\mathcal{B}_{k,i})_{k=1, \dots, m_i}$ for $i = 1, 2$, a family of open balls such that

$$0 < \epsilon \ll 1, \quad \mathcal{B}_{k,i} = B(P_{k,i}, \epsilon) \subset \Omega, \quad \text{and } \mathcal{B}_{k,i} \cap \mathcal{B}_{k',i} = \emptyset, \quad \text{if } k \neq k'. \quad (4)$$

1 Thus F vanishes as restricted to $\Omega_H = \Omega \setminus ((\cup_{k=1}^{m_1} \mathcal{B}_{k,1}) \cup (\cup_{k'=1}^{m_2} \mathcal{B}_{k',2}))$.

2 From the unique continuation theorem for the steady Stokes equation established in [11], we obtain $v = 0$
3 and $q = 0$ in Ω_H . Let us suppose that $m_1 > m_2$, and as the positions P_k are well separated and satisfy (2),
4 then there exists a source $P_{m_0,1} \neq P_{k',2}$, $k' = 1, \dots, m_2$, and we define $\Omega_0 = \Omega \setminus ((\cup_{k \neq m_0} \mathcal{B}_{k,1}) \cup (\cup_{k'=1}^{m_2} \mathcal{B}_{k',2}))$
5 with $k = 1, \dots, m_1$.

6 We denote $\mathcal{O} = \mathcal{B}_{m_0,1} \subset \Omega$. Thus, the solution (v, q) of the problem (\mathcal{P}) , which is null in $\Omega_0 \setminus \mathcal{O}$, satisfies
7 the following system in \mathcal{O} ;

$$\begin{cases} -\operatorname{div}(\sigma(v, q)) &= \lambda_{m_0,1} \delta_{P_{m_0,1}} & \text{in } \mathcal{O}, \\ \operatorname{div} v &= 0 & \text{in } \mathcal{O}, \\ v &= 0 & \text{on } \partial\mathcal{O}. \end{cases} \quad (5)$$

Let us consider now the solution (v_s, q_s) that satisfies:

$$\begin{cases} -\operatorname{div}(\sigma(v_s, q_s)) &= \lambda_{m_0,1} \delta_{P_{m_0,1}} & \text{in } \mathbb{R}^d, \\ \operatorname{div} v_s &= 0 & \text{in } \mathbb{R}^d, \end{cases}$$

and (v_r, q_r) which solves

$$\begin{cases} -\operatorname{div}(\sigma(v_r, q_r)) &= 0 & \text{in } \mathcal{O}, \\ \operatorname{div} v_r &= 0 & \text{in } \mathcal{O}, \\ v_r &= -v_s & \text{on } \partial\mathcal{O}. \end{cases}$$

Thus, the solution (v_s, q_s) is given by

$$(v_s, q_s) = (U * (\lambda_{m_0,1} \delta_{P_{m_0,1}}), P * (\lambda_{m_0,1} \delta_{P_{m_0,1}})) = (U(\cdot - P_{m_0,1}) \cdot \lambda_{m_0,1}, P(\cdot - P_{m_0,1}) \cdot \lambda_{m_0,1}),$$

where the pair (U, P) is the fundamental solution of the Stokes equation. It is given (see e.g. [2]), for $d = 2$,
by

$$\begin{cases} U_{ij}(x) &= \frac{1}{4\pi\nu} \left(\delta_{ij} \log\left(\frac{1}{|x|}\right) + \frac{x_i x_j}{|x|^2} \right), \quad i, j = 1, 2 \\ P_i(x) &= \frac{1}{2\pi} \frac{x_i}{|x|^2}, \quad i = 1, 2 \end{cases}$$

and, for $d = 3$,

$$\begin{cases} U_{ij}(x) &= \frac{1}{8\pi\nu} \left(\delta_{ij} \left(\frac{1}{|x|} + \frac{x_i x_j}{|x|^3} \right) \right), \quad i, j = 1, 2, 3 \\ P_i(x) &= \frac{1}{4\pi} \frac{x_i}{|x|^3}, \quad i = 1, 2, 3. \end{cases}$$

8 Then, we can deduce that the solution (v, q) of the problem (\mathcal{P}) , and which satisfies (5), can be written
9 $(v, q) = (v_r + v_s, q_r + q_s)$ in \mathcal{O} . Besides, we have (v_s, q_s) is an analytic solution in $\mathcal{O} \setminus P_{m_0,1}$, implies that v_s
10 is analytic on the boundary of \mathcal{O} , then v_r is an analytic function in $\mathcal{O} \setminus P_{m_0,1}$. Therefore, the fluid velocity
11 v , which is null in $\Omega_0 \setminus \mathcal{O}$, is an analytic function in $\mathcal{O} \setminus P_{m_0,1}$. This would imply that $\lambda_{m_0,1} = 0$, which by
12 assumption is impossible.

13 We proceed analogously, for the case $m_2 > m_1$. Thus, $m = m_1 = m_2$.
14

15 Now, let us suppose

$$\{P_{1,1}, \dots, P_{m,1}\} \neq \{P_{1,2}, \dots, P_{m,2}\},$$

and we assume that \mathcal{O} is a subset of Ω such that $\{\cup_{k=1}^m (P_{k,1} \cup P_{k,2})\} \in \mathcal{O}$. In the same way, we deduce that
the solution v is an analytic function in $\mathcal{O} \setminus \{\cup_{k=1}^m (P_{k,1} \cup P_{k,2})\}$, which is null in $\Omega \setminus \mathcal{O}$, and by application
of the unique continuation property we conclude that v equal to zero in \mathcal{O} , that is,

$$\sum_{k=1}^m (\lambda_{k,1} \delta_{P_{k,1}} - \lambda_{k,2} \delta_{P_{k,2}}) = 0 \text{ in } \mathcal{O},$$

such that $\lambda_{k,i} \neq 0$ for $k = 1, \dots, m_1$ and $i=1,2$. Therefore, there exists a unique permutation π of the entries such that,

$$P_{k,1} = P_{\pi(k),2}, \forall k = \{1, \dots, m\}.$$

1 Finally, we conclude that $F = \sum_{k=1}^m (\lambda_{k,1} - \lambda_{\pi(k),2}) \delta_{P_{k,2}}$. Using the same arguments, we obtain $\lambda_{k,1} = \lambda_{\pi(k),2}$,
 2 with $i=1,2$ and $k = 1, \dots, m$.

3 ■

4 3. A game formulation of the coupled data completion and point-forces identification problems

5 With the previous notations, let be $G \in H^{\frac{1}{2}}(\Gamma_c)^d$ and $\Phi \in (H_{00}^{\frac{1}{2}}(\Gamma_c)^d)'$ given Cauchy data. We recall that
 6 the inverse source-term problem amounts to find a collection of point-wise sources $F^* \in H^s(\Omega)^d$ for $s < -1$
 7 such that the fluid velocity u and the pressure p are solution to the following Cauchy-Stokes problem:

$$(\mathcal{CS}) \begin{cases} -\operatorname{div}(\sigma(u, p)) = F^* & \text{in } \Omega, \\ \operatorname{div} u = 0 & \text{in } \Omega, \\ u = G & \text{on } \Gamma_c, \\ \sigma(u, p)n = \Phi & \text{on } \Gamma_c. \end{cases}$$

8 For any given $\eta \in (H_{00}^{\frac{1}{2}}(\Gamma_i)^d)'$, $\tau \in H^{\frac{1}{2}}(\Gamma_i)^d$ and $F \in H^s(\Omega)^d$ for $s < -1$, we define the states $(u_1, p_1) =$
 9 $(u_1(\eta, F), p_1(\eta, F)) \in L^2(\Omega)^d \times L^2(\Omega)$ and $(u_2, p_2) = (u_2(\tau, F), p_2(\tau, F)) \in L^2(\Omega)^d \times L^2(\Omega)$ as the unique
 10 solution of the following Stokes mixed boundary value problem (\mathcal{P}_1) and (\mathcal{P}_2) ,

$$(\mathcal{P}_1) \begin{cases} -\operatorname{div}(\sigma(u_1, p_1)) = F & \text{in } \Omega, \\ \operatorname{div} u_1 = 0 & \text{in } \Omega, \\ u_1 = G & \text{on } \Gamma_c, \\ \sigma(u_1, p_1)n = \eta & \text{on } \Gamma_i, \end{cases} \quad (\mathcal{P}_2) \begin{cases} -\operatorname{div}(\sigma(u_2, p_2)) = F & \text{in } \Omega, \\ \operatorname{div} u_2 = 0 & \text{in } \Omega, \\ u_2 = \tau & \text{on } \Gamma_i, \\ \sigma(u_2, p_2)n = \Phi & \text{on } \Gamma_c. \end{cases}$$

11 The proof of the existence and uniqueness of the solutions to (\mathcal{P}_1) and (\mathcal{P}_2) , can be easily adapted from
 12 the proof given in [13] for the Dirichlet type boundary condition. Since the source F given by (1) belongs
 13 to Hilbert space $H^s(\Omega)^d$ with $s < -1$, a classical formulation of the problems (\mathcal{P}_1) and (\mathcal{P}_2) , well adapted
 14 to standard finite elements analysis is not possible. Nevertheless, to overcome this difficulty, we recourse to
 15 a relaxation technique, which consists in approximating the point-force support P_k by a small region, we
 16 could also use a subtraction method [2].

17 3.1. Relaxation step

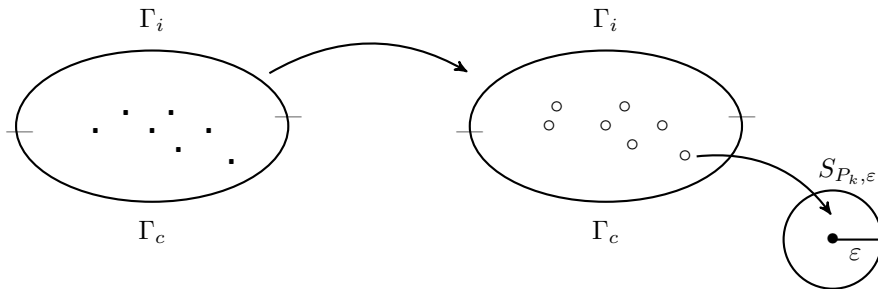


Figure 1: Relaxation step

We consider the classical approximation of a Dirac function at a points $P = \{P_1, \dots, P_m\}$ by the characteristic function of a small ball centred at P divided by its volume. Thus, instead of the source term F

given by (1), we consider the following:

$$F_\epsilon = \sum_{k=1}^m \frac{\lambda_k}{|\mathcal{S}_{P_k, \epsilon}|} \chi_{\mathcal{S}_{P_k, \epsilon}}$$

where $\chi_{\mathcal{S}_{P_k, \epsilon}}$ denotes the characteristic function of the ball $\mathcal{S}_{P_k, \epsilon} = P_k + \epsilon\omega_k$, with $\epsilon > 0$ is small enough and ω_k is bounded and smooth domain containing the origin. As the positions P_k are well separated and satisfy (2), we can suppose then that the region $\mathcal{S}_{P_k, \epsilon}$ also do not intersect,

$$\mathcal{S}_{P_k, \epsilon} \cap \mathcal{S}_{P_{k'}, \epsilon} = 0 \text{ if } k \neq k'. \quad (6)$$

The set of admissible source term \mathcal{D}_{ad} is defined by:

$$\mathcal{D}_{\text{ad}} = \left\{ f \in L^2(\Omega); f = \sum_{k=1}^p \beta_k \chi_{\mathcal{S}_{z_k, \epsilon}}, \text{ such that } \mathcal{S}_{z_k, \epsilon} \subset\subset \Omega \right\}.$$

Problems (\mathcal{P}_1) and (\mathcal{P}_2) are then rephrased in terms of this more regular source term. Let $(u_{1, \epsilon}, p_{1, \epsilon}) \in H^1(\Omega)^d \times L^2(\Omega)$ and $(u_{2, \epsilon}, p_{2, \epsilon}) \in H^1(\Omega)^d \times L^2(\Omega)$ be the unique solutions of the respective relaxed BVPs $(\mathcal{P}_{1, \epsilon})$ and $(\mathcal{P}_{2, \epsilon})$,

$$\begin{aligned} (\mathcal{P}_{1, \epsilon}) \quad & \begin{cases} -\operatorname{div}(\sigma(u_{1, \epsilon}, p_{1, \epsilon})) = F_\epsilon & \text{in } \Omega, \\ \operatorname{div} u_{1, \epsilon} = 0 & \text{in } \Omega, \\ u_{1, \epsilon} = G & \text{on } \Gamma_c, \\ \sigma(u_{1, \epsilon}, p_{1, \epsilon})n = \eta & \text{on } \Gamma_i, \end{cases} \\ (\mathcal{P}_{2, \epsilon}) \quad & \begin{cases} -\operatorname{div}(\sigma(u_{2, \epsilon}, p_{2, \epsilon})) = F_\epsilon & \text{in } \Omega, \\ \operatorname{div} u_{2, \epsilon} = 0 & \text{in } \Omega, \\ \sigma(u_{2, \epsilon}, p_{2, \epsilon})n = \Phi & \text{on } \Gamma_c, \\ u_{2, \epsilon} = \tau & \text{on } \Gamma_i, \end{cases} \end{aligned}$$

where

$$F_\epsilon = \sum_{k=1}^m \frac{\lambda_k}{|\mathcal{S}_{P_k, \epsilon}|} \chi_{\mathcal{S}_{P_k, \epsilon}} \in \mathcal{D}_{\text{ad}} \quad (7)$$

1 is more regular source term, with $\chi_{\mathcal{S}_{P_k, \epsilon}}$ is the characteristic function of the unknown region $\mathcal{S}_{P_k, \epsilon}$.

2 **Remark 1.** The existence and uniqueness of the solutions $(\mathcal{P}_{1, \epsilon})$ and $(\mathcal{P}_{2, \epsilon})$, can be derived from the general
3 theory on existence of solutions to the incompressible steady state Stokes equations, which can be found e.g.
4 in [8, 25]; See also [3] which is suitable to the Stokes framework of the present paper. Moreover, the solutions
5 $(u_{1, \epsilon}, p_{1, \epsilon})$ and $(u_{2, \epsilon}, p_{2, \epsilon})$ converge to the respective solutions (u_1, p_1) and (u_2, p_2) with the parameter ϵ , the
6 proof of this result can be handled by applying the same technique as in [13].

7
8 Let $\mathcal{I}_{\text{ad}} = \{(m; \lambda, P) \in \mathbb{N}^* \times \mathbb{R}^{dm} \times \Omega^m\}$. Let $\phi = (m; (\lambda_k, P_k)_{1 \leq k \leq m}) \in \mathcal{I}_{\text{ad}}$ be a source configuration
9 corresponding to a source F of the form (1). Let us introduce the following three cost functionals:

$$\mathcal{J}_1(\eta, \tau; \phi) = \frac{1}{2} \|\sigma(u_{1, \epsilon}, p_{1, \epsilon})n - \Phi\|_{(H_{00}^{\frac{1}{2}}(\Gamma_i)^d)'}^2 + \frac{\alpha}{2} \|u_{1, \epsilon} - u_{2, \epsilon}\|_{H^{\frac{1}{2}}(\Gamma_i)^d}^2, \quad (8)$$

$$\mathcal{J}_2(\eta, \tau; \phi) = \frac{1}{2} \|u_{2, \epsilon} - G\|_{H^{\frac{1}{2}}(\Gamma_c)^d}^2 + \frac{\alpha}{2} \|u_{1, \epsilon} - u_{2, \epsilon}\|_{H^{\frac{1}{2}}(\Gamma_i)^d}^2, \quad (9)$$

$$\mathcal{J}_3(\eta, \tau; \phi) = \|\sigma(u_{1, \epsilon}, p_{1, \epsilon}) - \sigma(u_{2, \epsilon}, p_{2, \epsilon})\|_{L^2(\Omega)^d}^2, \quad (10)$$

10 where α is given positive parameter (e.g. $\alpha = 1$). Player (1) controls the strategy variable $\eta \in (H_{00}^{\frac{1}{2}}(\Gamma_i)^d)'$
11 and aims at minimizing the cost \mathcal{J}_1 and Player (2) controls the strategy variable $\tau \in H^{\frac{1}{2}}(\Gamma_i)^d$ and aims at
12 minimizing the cost \mathcal{J}_2 : they are given Dirichlet (resp. Neumann) data and try to minimize the gap with
13 the Neumann (resp. Dirichlet) remaining condition. The player (3) controls the strategy variable $\phi \in \mathcal{I}_{\text{ad}}$
14 and aims at minimizing the Kohn-Vogelius type functional \mathcal{J}_3 .

1 **Definition 1.** A triplet $(\eta_N, \tau_N, \phi_N) \in (H_{00}^{\frac{1}{2}}(\Gamma_i)^d)' \times H^{\frac{1}{2}}(\Gamma_i)^d \times \mathcal{I}_{\text{ad}}$ is a Nash equilibrium for the three players
 2 game if the following holds:

$$\begin{cases} \mathcal{J}_1(\eta_N, \tau_N; \phi_N) \leq \mathcal{J}_1(\eta, \tau_N, \phi_N), & \forall \eta \in (H_{00}^{\frac{1}{2}}(\Gamma_i)^d)', \\ \mathcal{J}_2(\eta_N, \tau_N; \phi_N) \leq \mathcal{J}_2(\eta_N, \tau, \phi_N), & \forall \tau \in H^{\frac{1}{2}}(\Gamma_i)^d, \\ \mathcal{J}_3(\eta_N, \tau_N; \phi_N) \leq \mathcal{J}_3(\eta_N, \tau_N, \phi), & \forall \phi \in \mathcal{I}_{\text{ad}}. \end{cases} \quad (11)$$

3

The player 3 in charge of the inverse source-term problem has as a strategy $\phi = (m; (\lambda_k, P_k)_{1 \leq k \leq m})$, which is a solution of the following optimization problem,

$$\min_{\phi \in \mathcal{I}_{\text{ad}}} \mathcal{J}_3(\eta, \tau; \phi), \quad \text{when } (\eta, \tau) \in (H_{00}^{\frac{1}{2}}(\Gamma_i)^d)' \times H^{\frac{1}{2}}(\Gamma_i)^d.$$

4 In the following, the player (3) will play in two steps in order to determine the elements defining the
 5 source F introduced in (1); a first step enables to localize the source position $P = \{P_1, \dots, P_m\}$, or in other
 6 words after this relaxation step, the support of $\mathcal{S} = \cup_{k=1}^m \mathcal{S}_{k,\epsilon}$. Then, a second step uses the determined
 7 source position and compute the approximate value of the source intensity $\Lambda = \{\lambda_1, \dots, \lambda_m\}$.

8 3.2. Localization of the source position.

Here, the player (3) focuses on identifying the optimal location of the source-term with respect to the
 assumption (6). Therefore, the minimization problem of \mathcal{J}_3 w.r.t. P can be formulated as a topological op-
 timization one. Thus, the unknown region \mathcal{S} can be characterized as the solution to the following topological
 optimization problem, for fixed $(\eta, \tau, \Lambda) \in (H_{00}^{\frac{1}{2}}(\Gamma_i)^d)' \times H^{\frac{1}{2}}(\Gamma_i)^d \times \mathbb{R}^{dm}$,

$$\begin{cases} \text{Find } \mathcal{S}^* = \cup_{k=1}^m \mathcal{S}_{P_k, \epsilon} \subset \Omega, \text{ such that} \\ \mathcal{S}^* = \arg \min_{\mathcal{S} \subset \Omega} \left\{ \mathcal{J}(\mathcal{S}) := \int_{\Omega} |\sigma(u_{1,\epsilon}, p_{1,\epsilon}) - \sigma(u_{2,\epsilon}, p_{2,\epsilon})|^2 dx \right\}, \end{cases}$$

9 where $(u_{1,\epsilon}, p_{1,\epsilon})$ and $(u_{2,\epsilon}, p_{2,\epsilon})$ are the solutions to respectively $(\mathcal{P}_{1,\epsilon})$ and $(\mathcal{P}_{2,\epsilon})$. In order to solve this
 10 problem, we shall use a topological sensitivity analysis method. The concept of the topological derivative
 11 was proposed by Schumacher et al. [10] in the case of compliance minimization. Next, Sokolowski et al.
 12 [23] extended it to more general shape functionals. It consists of studying the variation of the cost function
 13 with respect to small perturbations of the domain's topology. It has been widely applied in literature for
 14 arbitrarily shaped perturbations and a general class of cost functionals related to PDEs. In our case, we
 15 want to apply the topological gradient computation to adding a source term of a given form to the Stokes
 16 equations. A topological gradient computation for a source term perturbation can be found in [13, 22].

17 3.2.1. Topological sensitivity method

This approach's main step consists of studying the variation of a given functional with respect to a small
 topological perturbation of the source term. For a given source term f , let $\delta f_{P,\epsilon}$ be a finite topological
 perturbation of f on the form

$$\delta f_{P,\epsilon} = \begin{cases} \lambda & \text{in } \omega_{P,\epsilon} = \cup_{k=1}^m \omega_{P_k,\epsilon} \\ 0 & \text{in } \Omega \setminus \overline{\cup_{k=1}^m \omega_{P_k,\epsilon}} \end{cases}$$

18 where $P = (P_1, \dots, P_m) \in \Omega^m$, and $\omega_{P_k,\epsilon}$, $1 \leq k \leq m$ are small geometrical perturbation separated and
 19 have the geometry form $\omega_{P_k,\epsilon} = P_k + \epsilon B$, where $\epsilon > 0$ is small enough and B is a fixed bounded domain
 20 containing the origin. The points $P_k \in \Omega$, $1 \leq k \leq m$, determine the location of the geometric $\omega_{P_k,\epsilon}$.

21

Then, the asymptotic expansion of the given cost function \mathcal{J} with respect to ϵ takes the form,

$$\begin{aligned} \mathcal{J}(f + \delta f_{P,\epsilon}) - \mathcal{J}(f) &= \rho(\epsilon) \sum_{k=1}^m \mathcal{G}(P_k) + o(\rho(\epsilon)), \quad \forall P_k \in \Omega, \\ \lim_{\epsilon \rightarrow 0} \rho(\epsilon) &= 0, \quad \rho(\epsilon) > 0, \end{aligned} \quad (12)$$

where the function \mathcal{G} is the so-called topological gradient. Therefore, the source location would be identified in the region where the topological gradient is the most negative, that means that, the function \mathcal{J} will be decreased if we add source terms at points P_k , $1 \leq k \leq m$.

Let us consider, for now, the case of a single support $\mathcal{S}_{x_0, \epsilon} := \omega_{x_0, \epsilon}$ such that the perturbation $\delta f_\epsilon := \delta f_{x_0, \epsilon}$ is given by

$$\delta f_\epsilon = \begin{cases} \lambda & \text{in } \mathcal{S}_{x_0, \epsilon}, \\ 0 & \text{in } \Omega \setminus \overline{\mathcal{S}_{x_0, \epsilon}}. \end{cases}$$

Then, we define the source function \mathcal{J} to be minimized,

$$\mathcal{J}(f + \delta f_\epsilon) := \mathcal{J}((u_1^\epsilon, p_1^\epsilon); (u_2^\epsilon, p_2^\epsilon)),$$

where

$$\mathcal{J}((u_1^\epsilon, p_1^\epsilon); (u_2^\epsilon, p_2^\epsilon)) = \int_{\Omega} |\sigma(u_1^\epsilon, p_1^\epsilon) - \sigma(u_2^\epsilon, p_2^\epsilon)|^2 dx,$$

and $(u_1^\epsilon, p_1^\epsilon)$ and $(u_2^\epsilon, p_2^\epsilon)$ are respective solutions of the following BVP,

$$(P_1^\epsilon) \begin{cases} -\operatorname{div}(\sigma(u_1^\epsilon, p_1^\epsilon)) = f + \delta f_\epsilon & \text{in } \Omega, \\ \operatorname{div} u_1^\epsilon = 0 & \text{in } \Omega, \\ u_1^\epsilon = G & \text{on } \Gamma_c, \\ \sigma(u_1^\epsilon, p_1^\epsilon)n = \eta & \text{on } \Gamma_i, \end{cases} \quad (P_2^\epsilon) \begin{cases} -\operatorname{div}(\sigma(u_2^\epsilon, p_2^\epsilon)) = f + \delta f_\epsilon & \text{in } \Omega, \\ \operatorname{div} u_2^\epsilon = 0 & \text{in } \Omega, \\ \sigma(u_2^\epsilon, p_2^\epsilon)n = \Phi & \text{on } \Gamma_c, \\ u_2^\epsilon = \tau & \text{on } \Gamma_i, \end{cases}$$

Then, the weak solutions to problem (P_1^ϵ) and (P_2^ϵ) are defined by:

$$\begin{cases} \text{Find } (u_1^\epsilon, p_1^\epsilon) \in H^1(\Omega)^d \times L^2(\Omega) \text{ such that,} \\ \mathcal{A}(u_1^\epsilon, \varphi_1) + \mathcal{B}(p_1^\epsilon, \varphi_1) = l_{1, \epsilon}(\varphi_1), \quad \forall \varphi_1 \in H_{\Gamma_c}^1(\Omega), \\ \mathcal{B}(\xi_1, u_1^\epsilon) = 0, \quad \forall \xi_1 \in L_0^2(\Omega), \end{cases} \quad (13)$$

$$\begin{cases} \text{Find } (u_2^\epsilon, p_2^\epsilon) \in H^1(\Omega)^d \times L^2(\Omega) \text{ such that,} \\ \mathcal{A}(u_2^\epsilon, \varphi_2) + \mathcal{B}(p_2^\epsilon, \varphi_2) = l_{2, \epsilon}(\varphi_2), \quad \forall \varphi_2 \in H_{\Gamma_c}^1(\Omega), \\ \mathcal{B}(\xi_2, u_2^\epsilon) = 0, \quad \forall \xi_2 \in L_0^2(\Omega), \end{cases} \quad (14)$$

where

$$\mathcal{A}(u_i^\epsilon, \varphi_i) = \int_{\Omega} D(u_i^\epsilon) : \nabla \varphi_i dx, \quad \mathcal{B}(p_i^\epsilon, \varphi_i) = - \int_{\Omega} p_i^\epsilon \operatorname{div} \varphi_i dx$$

and

$$l_{1, \epsilon}(\varphi_1) = \int_{\Omega} (f + \delta f_\epsilon) \varphi_1 dx + \int_{\Gamma_i} \eta \varphi_1 ds, \quad l_{2, \epsilon}(\varphi_2) = \int_{\Omega} (f + \delta f_\epsilon) \varphi_2 dx + \int_{\Gamma_c} \Phi \varphi_2 ds.$$

We now consider the case where $f = 0$, then, the linear forms $l_{1,0}$ and $l_{2,0}$ can be defined as follows

$$l_{1,0}(\varphi_1) = \int_{\Gamma_i} \eta \varphi_1 ds, \quad l_{2,0}(\varphi_2) = \int_{\Gamma_c} \Phi \varphi_2 ds.$$

1
2 Next, we introduce the following proposition which describes an adjoint method, for the computation of
3 this first variation of our cost function \mathcal{J} with respect to ϵ .

4 **Proposition 1.** Consider $(u_1^\epsilon, p_1^\epsilon)$ and $(u_2^\epsilon, p_2^\epsilon)$ solutions of the Problems (13) and (14), respectively. Sup-
5 pose that the following assumptions hold:

6 (i) \mathcal{J} is Fréchet-differentiable with respect to (u_i, p_i) , for $i = 1, 2$.
7

(ii) There exist two real numbers δl_1 and δl_2 such that

$$(l_{1,\epsilon} - l_{1,0})(v_1) = \rho(\epsilon)\delta l_1 + o(\rho(\epsilon)),$$

$$(l_{2,\epsilon} - l_{2,0})(v_2) = \rho(\epsilon)\delta l_2 + o(\rho(\epsilon)),$$

where (v_1, q_1) and (v_2, q_2) are solutions of the following weak formulations adjoint problems,

$$(\mathcal{AP}_1) \left\| \begin{aligned} \mathcal{A}(h_1, v_1) + \mathcal{B}(k_1, v_1) - \mathcal{B}(q_1, h_1) &= -\frac{\partial \mathcal{J}}{\partial u_1}((u_1^0, p_1^0); (u_2^0, p_2^0)).h_1 - \frac{\partial \mathcal{J}}{\partial p_1}((u_1^0, p_1^0); (u_2^0, p_2^0)).k_1 \end{aligned} \right.$$

$$(\mathcal{AP}_2) \left\| \begin{aligned} \mathcal{A}(h_2, v_2) + \mathcal{B}(k_2, v_2) - \mathcal{B}(q_2, h_2) &= -\frac{\partial \mathcal{J}}{\partial u_2}((u_1^0, p_1^0); (u_2^0, p_2^0)).h_2 - \frac{\partial \mathcal{J}}{\partial p_2}((u_1^0, p_1^0); (u_2^0, p_2^0)).k_2 \end{aligned} \right.$$

for all $(h_1, k_1) \in H_{\Gamma_c}^1(\Omega) \times L^2(\Omega)$ and $(h_2, k_2) \in H_{\Gamma_i}^1(\Omega) \times L^2(\Omega)$.

Then the first variation of the cost function \mathcal{J} with respect to ϵ is given by,

$$\mathcal{J}(\delta f_\epsilon) = \mathcal{J}(0) + \rho(\epsilon)(\delta l_1 + \delta l_2) + o(\rho(\epsilon)),$$

where $\rho(\epsilon) = |\mathcal{S}_{x_0, \epsilon}|$. The topological gradient \mathcal{G} at point x_0 is given by:

$$\mathcal{G}(x_0) = -\lambda.(v_1 + v_2)(x_0), \quad (15)$$

where λ is a constant vector and (v_i, q_i) is the solution of the adjoint problem (\mathcal{AP}_i) , with $i=1,2$.

Proof. Let us define the Lagrangian \mathcal{L} by,

$$\begin{aligned} \mathcal{L}_\epsilon(v_1, q_1, v_2, q_2, u_1, p_1, u_2, p_2) &= \mathcal{J}((u_1, p_1); (u_2, p_2)) + \mathcal{A}(u_1, v_1) + \mathcal{B}(p_1, v_1) \\ &\quad - \mathcal{B}(q_1, u_1) - l_{1,\epsilon}(v_1) + \mathcal{A}(u_2, v_2) + \mathcal{B}(p_2, v_2) - \mathcal{B}(q_2, u_2) - l_{2,\epsilon}(v_2), \end{aligned}$$

with $(u_1, u_2, v_1, v_2) \in H^1(\Omega)^d \times H^1(\Omega)^d \times H_{\Gamma_c}^1(\Omega) \times H_{\Gamma_i}^1(\Omega)$ and $(p_1, p_2, q_1, q_2) \in L^2(\Omega)^4$. Using (13) and (14), we obtain

$$\mathcal{J}(\delta f_\epsilon) = \mathcal{L}_\epsilon(v_1, q_1, v_2, q_2, u_1^\epsilon, p_1^\epsilon, u_2^\epsilon, p_2^\epsilon).$$

So the first variation of the cost function with respect to ϵ is given by:

$$\begin{aligned} \mathcal{J}(\delta f_\epsilon) - \mathcal{J}(0) &= \mathcal{L}_\epsilon(v_1, q_1, v_2, q_2, u_1^\epsilon, p_1^\epsilon, u_2^\epsilon, p_2^\epsilon) - \mathcal{L}_0(v_1, q_1, v_2, q_2, u_1^0, p_1^0, u_2^0, p_2^0) \\ &= \mathcal{A}(u_1^\epsilon, v_1) + \mathcal{B}(p_1^\epsilon, v_1) - \mathcal{B}(q_1, u_1^\epsilon) - \mathcal{A}(u_1^0, v_1) - \mathcal{B}(p_1^0, v_1) + \mathcal{B}(q_1, u_1^0) \\ &\quad + \mathcal{A}(u_2^\epsilon, v_2) + \mathcal{B}(p_2^\epsilon, v_2) - \mathcal{B}(q_2, u_2^\epsilon) - \mathcal{A}(u_2^0, v_2) - \mathcal{B}(p_2^0, v_2) + \mathcal{B}(q_2, u_2^0) \\ &\quad - (l_1^\epsilon - l_1^0)(v_1) - (l_2^\epsilon - l_2^0)(v_2) + \mathcal{J}((u_1^\epsilon, p_1^\epsilon); (u_2^\epsilon, p_2^\epsilon)) - \mathcal{J}((u_1^0, p_1^0); (u_2^0, p_2^0)) \end{aligned}$$

Then, from the definition of \mathcal{A} and \mathcal{B} , we have

$$\begin{aligned} &\mathcal{A}(u_1^\epsilon, v_1) + \mathcal{B}(p_1^\epsilon, v_1) - \mathcal{B}(q_1, u_1^\epsilon) - \mathcal{A}(u_1^0, v_1) - \mathcal{B}(p_1^0, v_1) \\ &\quad + \mathcal{B}(q_1, u_1^0) = \int_{\Omega} D(u_1^\epsilon - u_1^0) : \nabla v_1 \, dx + \int_{\Omega} (p_1^\epsilon - p_1^0) \operatorname{div} v_1 \, dx - \int_{\Omega} q_1 \operatorname{div} (u_1^\epsilon - u_1^0) \, dx, \\ &\mathcal{A}(u_2^\epsilon, v_2) + \mathcal{B}(p_2^\epsilon, v_2) - \mathcal{B}(q_2, u_2^\epsilon) - \mathcal{A}(u_2^0, v_2) - \mathcal{B}(p_2^0, v_2) \\ &\quad + \mathcal{B}(q_2, u_2^0) = \int_{\Omega} D(u_2^\epsilon - u_2^0) : \nabla v_2 \, dx + \int_{\Omega} (p_2^\epsilon - p_2^0) \operatorname{div} v_2 \, dx - \int_{\Omega} q_2 \operatorname{div} (u_2^\epsilon - u_2^0) \, dx. \end{aligned}$$

Choosing (v_1, q_1) and (v_2, q_2) as the solutions of the adjoints problems (\mathcal{AP}_1) and (\mathcal{AP}_2) ,

$$\begin{aligned}
& \int_{\Omega} D(u_1^\epsilon - u_1^0) : \nabla v_1 dx + \int_{\Omega} (p_1^\epsilon - p_1^0) \operatorname{div} v_1 dx - \int_{\Omega} q_1 \operatorname{div} (u_1^\epsilon - u_1^0) dx = \\
& \quad - \frac{\partial \mathcal{J}}{\partial u_1}((u_1^0, p_1^0); (u_2^0, p_2^0)) \cdot (u_1^\epsilon - u_1^0) - \frac{\partial \mathcal{J}}{\partial p_1}((u_1^0, p_1^0); (u_2^0, p_2^0)) \cdot (p_1^\epsilon - p_1^0), \\
& \int_{\Omega} D(u_2^\epsilon - u_2^0) : \nabla v_2 dx + \int_{\Omega} (p_2^\epsilon - p_2^0) \operatorname{div} v_2 dx - \int_{\Omega} q_2 \operatorname{div} (u_2^\epsilon - u_2^0) dx = \\
& \quad - \frac{\partial \mathcal{J}}{\partial u_2}((u_1^0, p_1^0); (u_2^0, p_2^0)) \cdot (u_2^\epsilon - u_2^0) - \frac{\partial \mathcal{J}}{\partial p_2}((u_1^0, p_1^0); (u_2^0, p_2^0)) \cdot (p_2^\epsilon - p_2^0).
\end{aligned}$$

1 Thus, we have

$$\begin{aligned}
\mathcal{J}(\delta f_\epsilon) - \mathcal{J}(0) &= - \frac{\partial \mathcal{J}}{\partial u_1}((u_1^0, p_1^0); (u_2^0, p_2^0)) \cdot (u_1^\epsilon - u_1^0) - \frac{\partial \mathcal{J}}{\partial p_1}((u_1^0, p_1^0); (u_2^0, p_2^0)) \cdot (p_1^\epsilon - p_1^0) \\
&\quad - \frac{\partial \mathcal{J}}{\partial u_2}((u_1^0, p_1^0); (u_2^0, p_2^0)) \cdot (u_2^\epsilon - u_2^0) - \frac{\partial \mathcal{J}}{\partial p_2}((u_1^0, p_1^0); (u_2^0, p_2^0)) \cdot (p_2^\epsilon - p_2^0) \\
&\quad - (l_1^\epsilon - l_1^0)(v_1) - (l_2^\epsilon - l_2^0)(v_2) + \mathcal{J}((u_1^\epsilon, p_1^\epsilon); (u_2^\epsilon, p_2^\epsilon)) - \mathcal{J}((u_1^0, p_1^0); (u_2^0, p_2^0))
\end{aligned}$$

• *Variation of the linear form.* We are interested here in the asymptotic analysis of the variation

$$\begin{aligned}
(l_{1,\epsilon} - l_{1,0})(v_1) &= \int_{\Omega} \delta f_\epsilon v_1 dx = \int_{\mathcal{S}_{x_0,\epsilon}} \lambda v_1 dx, \\
&= |\mathcal{S}_{x_0,\epsilon}| \lambda v_1(x_0) + o(\epsilon).
\end{aligned} \tag{16}$$

where (v_1, q_1) is the solution of the adjoint problem (\mathcal{AP}_1) . The same, we have

$$(l_{2,\epsilon} - l_{2,0})(v_2) = |\mathcal{S}_{x_0,\epsilon}| \lambda v_2(x_0) + o(\epsilon), \tag{17}$$

2 where (v_2, q_2) is the solution of the adjoint problem (\mathcal{AP}_2) .

3

• *Variation of the cost function.* Let us now turn to the asymptotic analysis of the variation of the Kohn-Vogelius functional given by

$$\mathcal{J}((u_1^\epsilon, p_1^\epsilon); (u_2^\epsilon, p_2^\epsilon)) = \int_{\Omega} |\sigma(u_1^\epsilon, p_1^\epsilon) - \sigma(u_2^\epsilon, p_2^\epsilon)|^2 dx.$$

Thus, this functional \mathcal{J} can be decomposed as

$$\mathcal{J}((u_1^\epsilon, p_1^\epsilon); (u_2^\epsilon, p_2^\epsilon)) = \mathfrak{J}_1(u_1^\epsilon, p_1^\epsilon) + \mathfrak{J}_2(u_2^\epsilon, p_2^\epsilon) - 2\mathfrak{J}_{12}(u_1^\epsilon, p_1^\epsilon; u_2^\epsilon, p_2^\epsilon),$$

4 with

$$\mathfrak{J}_1(u_1^\epsilon, p_1^\epsilon) = \int_{\Omega} |\sigma(u_1^\epsilon, p_1^\epsilon)|^2 dx,$$

$$\mathfrak{J}_2(u_2^\epsilon, p_2^\epsilon) = \int_{\Omega} |\sigma(u_2^\epsilon, p_2^\epsilon)|^2 dx,$$

$$\mathfrak{J}_{12}((u_1^\epsilon, p_1^\epsilon); (u_2^\epsilon, p_2^\epsilon)) = \int_{\Omega} \sigma(u_1^\epsilon, p_1^\epsilon) \sigma(u_2^\epsilon, p_2^\epsilon) dx.$$

Variation of \mathfrak{J}_1 :

$$\begin{aligned}
\mathfrak{J}_1(u_1^\epsilon, p_1^\epsilon) - \mathfrak{J}_1(u_1^0, p_1^0) &= \int_{\Omega} |\sigma(u_1^\epsilon, p_1^\epsilon)|^2 dx - \int_{\Omega} |\sigma(u_1^0, p_1^0)|^2 dx \pm 2 \int_{\Omega} |\sigma(u_1^0, p_1^0)|^2 dx \\
&= \int_{\Omega} |\sigma(u_1^\epsilon, p_1^\epsilon) - \sigma(u_1^0, p_1^0)|^2 dx + 2 \int_{\Omega} \sigma(u_1^\epsilon, p_1^\epsilon) \sigma(u_1^0, p_1^0) dx - 2 \int_{\Omega} |\sigma(u_1^0, p_1^0)|^2 dx.
\end{aligned}$$

Posing $(w_i^\epsilon, \xi_i^\epsilon) = (u_i^\epsilon - u_i^0, p_i^\epsilon - p_i^0)$ for $i=1,2$, we obtain

$$\mathfrak{J}_1(u_1^\epsilon, p_1^\epsilon) - \mathfrak{J}_1(u_1^0, p_1^0) = \int_{\Omega} |\sigma(w_1^\epsilon, \xi_1^\epsilon)|^2 dx + 2 \int_{\Omega} \sigma(u_1^0, p_1^0) \sigma(w_1^\epsilon, \xi_1^\epsilon) dx. \quad (18)$$

Variation of \mathfrak{J}_2 : In the same way, we find that

$$\mathfrak{J}_2(u_2^\epsilon, p_2^\epsilon) - \mathfrak{J}_2(u_2^0, p_2^0) = \int_{\Omega} |\sigma(w_2^\epsilon, \xi_2^\epsilon)|^2 dx + 2 \int_{\Omega} \sigma(u_2^0, p_2^0) \sigma(w_2^\epsilon, \xi_2^\epsilon) dx. \quad (19)$$

1 *Variation of \mathfrak{J}_{12} :*

$$\mathfrak{J}_{12}((u_1^\epsilon, p_1^\epsilon); (u_2^\epsilon, p_2^\epsilon)) - \mathfrak{J}_{12}((u_1^0, p_1^0); (u_2^0, p_2^0)) = \int_{\Omega} \sigma(u_1^\epsilon, p_1^\epsilon) \sigma(u_2^\epsilon, p_2^\epsilon) dx - \int_{\Omega} \sigma(u_1^0, p_1^0) \sigma(u_2^0, p_2^0) dx.$$

Then, we have

$$\begin{aligned} \mathfrak{J}_{12}((u_1^\epsilon, p_1^\epsilon); (u_2^\epsilon, p_2^\epsilon)) - \mathfrak{J}_{12}((u_1^0, p_1^0); (u_2^0, p_2^0)) &= \int_{\Omega} \sigma(w_1^\epsilon, \xi_1^\epsilon) \sigma(w_2^\epsilon, \xi_2^\epsilon) dx \\ &+ \int_{\Omega} \sigma(u_1^0, p_1^0) \sigma(w_2^\epsilon, \xi_2^\epsilon) dx + \int_{\Omega} \sigma(u_2^0, p_2^0) \sigma(w_1^\epsilon, \xi_1^\epsilon) dx \end{aligned} \quad (20)$$

Combining the variations (18), (19) and (20), we obtain

$$\begin{aligned} \mathcal{J}((u_1^\epsilon, p_1^\epsilon); (u_2^\epsilon, p_2^\epsilon)) - \mathcal{J}((u_1^0, p_1^0); (u_2^0, p_2^0)) &= \int_{\Omega} |\sigma(w_1^\epsilon, \xi_1^\epsilon)|^2 dx + \int_{\Omega} |\sigma(w_2^\epsilon, \xi_2^\epsilon)|^2 dx \\ &- 2 \int_{\Omega} \sigma(w_1^\epsilon, \xi_1^\epsilon) \sigma(w_2^\epsilon, \xi_2^\epsilon) dx + 2 \int_{\Omega} (\sigma(u_1^0, p_1^0) - \sigma(u_2^0, p_2^0)) \sigma(w_1^\epsilon, \xi_1^\epsilon) dx \\ &- 2 \int_{\Omega} (\sigma(u_1^0, p_1^0) - \sigma(u_2^0, p_2^0)) \sigma(w_2^\epsilon, \xi_2^\epsilon) dx. \end{aligned}$$

Therefore,

$$\begin{aligned} \mathcal{J}((u_1^\epsilon, p_1^\epsilon); (u_2^\epsilon, p_2^\epsilon)) - \mathcal{J}((u_1^0, p_1^0); (u_2^0, p_2^0)) &- \frac{\partial \mathcal{J}}{\partial u_1}((u_1^0, p_1^0); (u_2^0, p_2^0)) \cdot w_1^\epsilon \\ &- \frac{\partial \mathcal{J}}{\partial p_1}((u_1^0, p_1^0); (u_2^0, p_2^0)) \cdot \xi_1^\epsilon - \frac{\partial \mathcal{J}}{\partial u_2}((u_1^0, p_1^0); (u_2^0, p_2^0)) \cdot w_2^\epsilon \\ &- \frac{\partial \mathcal{J}}{\partial p_2}((u_1^0, p_1^0); (u_2^0, p_2^0)) \cdot \xi_2^\epsilon = \mathcal{I}(\epsilon), \end{aligned}$$

where

$$\mathcal{I}(\epsilon) = \|\sigma(w_1^\epsilon, \xi_1^\epsilon)\|_{0,\Omega}^2 + \|\sigma(w_2^\epsilon, \xi_2^\epsilon)\|_{0,\Omega}^2 - 2 \int_{\Omega} \sigma(w_1^\epsilon, \xi_1^\epsilon) \sigma(w_2^\epsilon, \xi_2^\epsilon) dx.$$

We will then prove that $\mathcal{I}(\epsilon) = o(\rho(\epsilon))$. Thus, the topological asymptotic expansion of the functional \mathcal{J} with respect to ϵ is given by

$$\mathcal{J}(\delta f_\epsilon) - \mathcal{J}(0) = -|\mathcal{S}_{x_0, \epsilon}| \lambda(v_1 + v_2)(x_0) + o(|\mathcal{S}_{x_0, \epsilon}|),$$

then the topological gradient \mathcal{G} at point x_0 is given by

$$\mathcal{G}(x_0) = -\lambda(v_1 + v_2)(x_0).$$

2 Let's now show that $\mathcal{I}(\epsilon) = o(|\mathcal{S}_{x_0, \epsilon}|)$. Consider $(w_1^\epsilon, \xi_1^\epsilon) = (u_1^\epsilon - u_1^0, p_1^\epsilon - p_1^0)$ solution of the following
3 problem,

$$\begin{cases} -\operatorname{div}(\sigma(w_1^\epsilon, \xi_1^\epsilon)) &= \delta f_\epsilon & \text{in } \Omega, \\ \operatorname{div} w_1^\epsilon &= 0 & \text{in } \Omega, \\ w_1^\epsilon &= 0 & \text{on } \Gamma_c, \\ \sigma(w_1^\epsilon, \xi_1^\epsilon) n &= 0 & \text{on } \Gamma_i. \end{cases}$$

1 This problem is well-posed and has a unique solution in $H^1(\Omega)^d \times L^2(\Omega)$, see e.g. [5]. Using ([3], theorem 5.2),
 2 there exists a positive constant C such that,

$$\begin{aligned} \|w_1^\epsilon\|_{1,\Omega} + \|\xi_1^\epsilon\|_{0,\Omega} &\leq C\|\delta f_\epsilon\|_{0,\Omega} \\ &\leq C\|\lambda\|(\rho(\epsilon))^{\frac{1}{2}}. \end{aligned} \quad (21)$$

3 The same for the solution $(w_2^\epsilon, \xi_2^\epsilon)$. Using these latter results, we obtain an estimation of the third term of
 4 \mathcal{I} . We deduce then that $\mathcal{I}(\epsilon) = o(\rho(\epsilon))$. ■

6 3.3. Identification of the source intensity.

In this subsection, the player (3) assumes to be known the position $P = x_0$ defining a source-term F_ϵ that satisfies (7) and focuses on identifying the source intensity λ_k . To this end, player (3) must minimize the functional \mathcal{J}_3 with respect to λ . So the source intensity can be characterized as the solution of the following minimization problem,

$$\lambda^* = \arg \min_{\lambda \in \mathbb{R}^d} \left\{ \mathcal{J}_3(\eta, \tau; \phi) := \int_{\Omega} |\sigma(u_{1,\epsilon}, p_{1,\epsilon}) - \sigma(u_{2,\epsilon}, p_{2,\epsilon})|^2 dx \right\},$$

7 where $(u_{1,\epsilon}, p_{1,\epsilon})$ and $(u_{2,\epsilon}, p_{2,\epsilon})$ solve respectively problems $(\mathcal{P}_{1,\epsilon})$ and $(\mathcal{P}_{2,\epsilon})$. In order to perform the partial
 8 optimization problem of $\mathcal{J}_3(\eta, \tau; \phi)$ w.r.t the source intensity λ with (η, τ) given by players (1) and (2), one
 9 needs to compute the derivative of \mathcal{J}_3 w.r.t. λ . We have the following:

Proposition 2. *We have the following partial derivative,*

$$\frac{\partial \mathcal{J}_3}{\partial \lambda} \cdot \varphi = -\frac{1}{|\mathcal{S}_{x_0, \epsilon}|} \int_{\mathcal{S}_{x_0, \epsilon}} (z_1 + z_2)(x) \cdot \varphi dx, \quad \forall \varphi \in \mathbb{R},$$

10 where $(z_1, \pi_1) \in H_{\Gamma_c}^1(\Omega) \times L^2(\Omega)$ and $(z_2, \pi_2) \in H_{\Gamma_i}^1(\Omega) \times L^2(\Omega)$ are respective solutions of the adjoints
 11 problems,

$$\left\{ \begin{array}{l} 2 \int_{\Omega} (\sigma(u_{1,\epsilon}, p_{1,\epsilon}) - \sigma(u_{2,\epsilon}, p_{2,\epsilon})) : (\nabla h_1 + \nabla h_1^T) dx - \int_{\Omega} \pi_1 \operatorname{div} h_1 dx \\ \quad + \int_{\Omega} ((\nabla h_1 + \nabla h_1^T) : \nabla z_1) dx = 0, \quad \forall h_1 \in H_{\Gamma_c}^1(\Omega), \\ -2 \int_{\Omega} (\sigma(u_{1,\epsilon}, p_{1,\epsilon}) - \sigma(u_{2,\epsilon}, p_{2,\epsilon})) : (k_1 I_d) dx - \int_{\Omega} k_1 \operatorname{div} z_1 dx = 0, \\ \quad \forall k_1 \in L^2(\Omega), \end{array} \right. \quad (22)$$

$$\left\{ \begin{array}{l} -2 \int_{\Omega} (\sigma(u_{1,\epsilon}, p_{1,\epsilon}) - \sigma(u_{2,\epsilon}, p_{2,\epsilon})) : (\nabla h_2 + \nabla h_2^T) dx - \int_{\Omega} \pi_2 \operatorname{div} h_2 dx \\ \quad + \int_{\Omega} ((\nabla h_2 + \nabla h_2^T) : \nabla z_2) dx = 0, \quad \forall h_2 \in H_{\Gamma_i}^1(\Omega), \\ 2 \int_{\Omega} (\sigma(u_{1,\epsilon}, p_{1,\epsilon}) - \sigma(u_{2,\epsilon}, p_{2,\epsilon})) : (k_2 I_d) dx - \int_{\Omega} k_2 \operatorname{div} z_2 dx = 0, \\ \quad \forall k_2 \in L^2(\Omega), \end{array} \right. \quad (23)$$

12 and where $(u_{1,\epsilon}, p_{1,\epsilon})$ and $(u_{2,\epsilon}, p_{2,\epsilon})$ are the solutions to respectively $(\mathcal{P}_{1,\epsilon})$ and $(\mathcal{P}_{2,\epsilon})$.

13 3.4. The three-player Nash algorithm

14 We are now ready to state the three-player identification/completion Nash game. As aforementioned,
 15 players (1) and (2) aim at solving the Cauchy problem, while player (3) is aimed at minimizing a Kohn-
 16 Vogelius type energy, intended to identify the elements of the source-term. The game is of Nash type, which
 17 means that it is static with complete information [15] and hence its solution is a Nash equilibrium (NE), see
 18 Definition 1.

1 Given a triplet $(\eta, \tau; \phi) \in (H_{00}^{\frac{1}{2}}(\Gamma_i)^d)' \times H^{\frac{1}{2}}(\Gamma_i)^d \times \mathcal{I}_{\text{ad}}$, and we define $(u_{1,\epsilon}, p_{1,\epsilon}) := (u_{1,\epsilon}(\eta, \phi), p_{1,\epsilon}(\eta, \phi))$
2 be the solution to the approximate Stokes problem $(\mathcal{P}_{1,\epsilon})$ and $(u_{2,\epsilon}, p_{2,\epsilon}) := (u_{2,\epsilon}(\tau, \phi), p_{2,\epsilon}(\tau, \phi))$ the solution
3 to the approximate Stokes problem $(\mathcal{P}_{2,\epsilon})$, then the three players and their respective costs are defined as
4 follows:

- Player (1) has control on the Neumann strategies $\eta \in (H_{00}^{\frac{1}{2}}(\Gamma_i)^d)'$, and its cost functional is given by

$$\mathcal{J}_1(\eta, \tau; \phi) = \frac{1}{2} \|\sigma(u_{1,\epsilon}, p_{1,\epsilon})n - \Phi\|_{(H_{00}^{\frac{1}{2}}(\Gamma_c)^d)'}^2 + \frac{1}{2} \|u_{1,\epsilon} - u_{2,\epsilon}\|_{H^{\frac{1}{2}}(\Gamma_i)^d}^2. \quad (24)$$

- Player (2) has control on the Dirichlet strategies $\tau \in H^{\frac{1}{2}}(\Gamma_i)^d$, and its cost functional is given by

$$\mathcal{J}_2(\eta, \tau; \phi) = \frac{1}{2} \|u_{2,\epsilon} - f\|_{H^{\frac{1}{2}}(\Gamma_c)^d}^2 + \frac{1}{2} \|u_{1,\epsilon} - u_{2,\epsilon}\|_{H^{\frac{1}{2}}(\Gamma_i)^d}^2. \quad (25)$$

- Player (3) has control on the elements $\phi \in \mathcal{I}_{\text{ad}}$ defining the unknown source, and its cost functional is given by

$$\mathcal{J}_3(\eta, \tau; \phi) = \int_{\Omega} |\sigma(u_{1,\epsilon}, p_{1,\epsilon}) - \sigma(u_{2,\epsilon}, p_{2,\epsilon})|^2 dx. \quad (26)$$

5
6
7 In algorithm 1 below, we describe the main steps in computing the Nash equilibrium, with a version
8 where the Cauchy data of the Dirichlet type G are possibly perturbed by a noise with some magnitude σ ,
9 yielding for the Cauchy problem a noisy Dirichlet data G^σ .

10
11
12
13 The topological gradient and the gradient with fixed step methods are used to solve step I and II,
14 respectively, in the Algorithm 1. In step II, in order to solve the problems of partial optimization of \mathcal{J}_1 , \mathcal{J}_2
15 and \mathcal{J}_3 , we need to calculate the gradient of these costs with respect to their respective strategies η , τ and
16 λ . The fast computation of the latter is classical, and led by means of an adjoint state method, as shown
17 by the proposition 2 and 3, the proof of the proposition 3 is given in ([16], Appendix A. 1).

18 **Proposition 3.** [16] *We have the following two partial derivatives:*

$$\left\{ \begin{array}{l} \frac{\partial \mathcal{J}_1}{\partial \eta} \cdot \psi = - \int_{\Gamma_c} \psi \lambda_1 ds, \quad \forall \psi \in (H_{00}^{\frac{1}{2}}(\Gamma_i)^d)', \\ \text{with } (\lambda_1, \kappa_1) \in H_{\Gamma_c}^1(\Omega) \times L^2(\Omega) \quad \text{solution of the adjoint problem:} \\ \left\{ \begin{array}{l} \int_{\Gamma_c} (\sigma(u_{1,\epsilon}, p_{1,\epsilon})n - \Phi)((\nabla \gamma + \nabla \gamma^T)n) ds + \int_{\Gamma_c} (u_{1,\epsilon} - u_{2,\epsilon}) \gamma ds \\ \quad + \int_{\Omega} (\nabla \gamma + \nabla \gamma^T) : \nabla \lambda_1 dx - \int_{\Omega} \kappa_1 \text{div} \gamma dx = 0, \quad \forall \gamma \in H_{\Gamma_c}^1(\Omega), \\ - \int_{\Gamma_c} (\sigma(u_{1,\epsilon}, p_{1,\epsilon})n - \Phi) \delta n ds - \int_{\Omega} \delta \text{div} \lambda_1 dx = 0, \quad \forall \delta \in L^2(\Omega), \end{array} \right. \end{array} \right. \quad (27)$$

$$\left\{ \begin{array}{l} \frac{\partial \mathcal{J}_2}{\partial \tau} \cdot \mu = \int_{\Gamma_c} (\sigma(\lambda_2, \kappa_2)n - (u_{1,\epsilon} - u_{2,\epsilon})) \mu ds, \quad \forall \mu \in H^{\frac{1}{2}}(\Gamma_i)^d, \\ \text{with } (\lambda_2, \kappa_2) \in H^1(\Omega)^d \times L^2(\Omega) \quad \text{solution of the adjoint problem:} \\ \left\{ \begin{array}{l} \int_{\Omega} (\nabla \lambda_2 + \nabla \lambda_2^T) : \nabla \varphi dx - \int_{\Omega} \kappa_2 \text{div} \varphi dx = \int_{\Gamma_c} (G - u_{2,\epsilon}) \varphi ds, \\ \quad \forall \varphi \in H_{\Gamma_c}^1(\Omega), \\ \int_{\Omega} \xi \text{div} \lambda_2 dx = 0, \quad \forall \xi \in L^2(\Omega), \end{array} \right. \end{array} \right. \quad (28)$$

19 where, by a classical convention, $\nabla u : \nabla v = \text{Tr}(\nabla u \nabla v^T) = \sum_{i,j} \frac{\partial u_i}{\partial x_j} \frac{\partial v_i}{\partial x_j}$.

Algorithm 1: Computation of the Nash equilibrium (η_N, τ_N, ϕ_N)

Data: $\epsilon_S > 0$ a convergence tolerance, K_{max} a computational budget per Nash iteration, N_{max} a maximum Nash iterations and ϱ a-tuned-function which depends on the noise.

Set $n = 0$, choose an initial source intensity $\lambda^{(0)}$ and $F_\epsilon = 0$;

while $\|u_2 - G\|_{0,\Gamma_c} > \varrho$ **do**

Set $k = 0$ and choose an initial guess $(\eta^{(0)}, \tau^{(0)}) \in (H_{00}^{\frac{1}{2}}(\Gamma_i)^d)' \times H^{\frac{1}{2}}(\Gamma_i)^d$;

Compute $\bar{\eta}^{(k)}$ solution of $\min_{\eta} \mathcal{J}_1(\eta, \tau^{(k)}; F_\epsilon)$.

Compute (in parallel) $\bar{\tau}^{(k)}$ solution of $\min_{\tau} \mathcal{J}_2(\eta^{(k)}, \tau; F_\epsilon)$.

Evaluate $(\eta^{(k+1)}, \tau^{(k+1)}) = \alpha(\eta^{(k)}, \tau^{(k)}) + (1 - \alpha)(\bar{\eta}^{(k)}, \bar{\tau}^{(k)})$, with $0 \leq \alpha < 1$.

- Step I: Set $F_\epsilon = 0$, and use the one-shot algorithm to determine the set of optimal locations $P^{(n)} = \{P_1, \dots, P_{m^{(n)}}\}$:

- Solve two well-posed mixed forward problems:

$$\begin{aligned}
 (\mathcal{P}_1^0) \quad & \left\{ \begin{array}{ll} -\operatorname{div}(\sigma(u_1^{0,k+1}, p_1^{0,k+1})) = 0 & \text{in } \Omega, \\ \operatorname{div} u_1^{0,k+1} = 0 & \text{in } \Omega, \\ u_1^{0,k+1} = G & \text{on } \Gamma_c, \\ \sigma(u_1^{0,k+1}, p_1^{0,k+1})n = \eta^{(k+1)} & \text{on } \Gamma_i, \end{array} \right. \\
 (\mathcal{P}_2^0) \quad & \left\{ \begin{array}{ll} -\operatorname{div}(\sigma(u_2^{0,k+1}, p_2^{0,k+1})) = 0 & \text{in } \Omega, \\ \operatorname{div} u_2^{0,k+1} = 0 & \text{in } \Omega, \\ \sigma(u_2^{0,k+1}, p_2^{0,k+1})n = \Phi & \text{on } \Gamma_c, \\ u_2^{0,k+1} = \tau^{(k+1)} & \text{on } \Gamma_i. \end{array} \right.
 \end{aligned}$$

- Solve the adjoint problems (\mathcal{AP}_1) and (\mathcal{AP}_2) with respective solutions v_1 and v_2 .
- Compute the topological gradient \mathcal{G} using Formula (15), i.e.

$$\mathcal{G}(x) = -\lambda^{(k)} \cdot (v_1 + v_2)(x), \quad \forall x \in \Omega.$$

- Seek

$$P^{(n)} = \arg \min_{x \in \Omega} \mathcal{J}_3(\eta^{(k+1)}, \tau^{(k+1)}; (\lambda^{(k)}, x)).$$

- Step II: Solve the Nash game between η , τ and λ : Set $k = 1$,

- Step 1: Evaluate $F_\epsilon^{(n,k)} = \sum_{i=1}^{m^{(n)}} \frac{1}{|\mathcal{S}_{P_i, \epsilon}|} \lambda_i^{(k-1)} \chi_{\mathcal{S}_{P_i, \epsilon}}$.
- Step 2: Compute $\bar{\eta}^{(k)}$ solution of $\min_{\eta} \mathcal{J}_1(\eta, \tau^{(k)}; (\lambda^{(k-1)}, P^{(n)}))$.
- Step 3: Compute (in parallel) $\bar{\tau}^{(k)}$ solution of $\min_{\tau} \mathcal{J}_2(\eta^{(k)}, \tau; (\lambda^{(k-1)}, P^{(n)}))$.
- Step 4: Compute (in parallel) $\bar{\lambda}^{(k)}$ solution of $\min_{\lambda} \mathcal{J}_3(\eta^{(k)}, \tau^{(k)}; (\lambda, P^{(n)}))$.
- Step 5: For $0 \leq \alpha < 1$, set

$$S^{(k+1)} = (\eta^{(k+1)}, \tau^{(k+1)}, \lambda^{(k)}) = \alpha(\eta^{(k)}, \tau^{(k)}, \lambda^{(k-1)}) + (1 - \alpha)(\bar{\eta}^{(k)}, \bar{\tau}^{(k)}, \bar{\lambda}^{(k)}).$$

While $\|S^{(k+1)} - S^{(k)}\| > \epsilon_S$ and $k < N_{max}$, set $k = k + 1$, return back to step 1.

end

4. Numerical experiments

In this section, we illustrate the numerical results obtained using the 3-costs functionals described in the previous section 3. In order to test the efficiency of the proposed numerical method, we solve the source Cauchy-Stokes problem in the 2-D situations: the annular domain and a geometry with corners are considered. Then, we present an example of numerical reconstruction in the three-dimensional 3-D case. In our numerical experiments, we use L2 norms to estimate errors and calculate the gradient of the cost functionals.

Given a known the elements defining the source term F_ϵ^* , that is $\phi^* = (\lambda, P)$, we solve the following Stokes problem :

$$\begin{cases} -\operatorname{div}(\sigma(u, p)) = F_\epsilon^* & \text{in } \Omega, \\ \operatorname{div} u = 0 & \text{in } \Omega, \\ u = G & \text{on } \Gamma_c, \\ \beta u + \gamma \sigma(u, p)n = \beta H + \gamma \Psi & \text{on } \Gamma_i, \end{cases} \quad (29)$$

where the (phantom) exact solution (u, p) is used to build the remaining Cauchy data $\Phi = \sigma(u, p)n|_{\Gamma_c}$, and the exact missing data $u|_{\Gamma_i}$ and $\sigma(u, p)n|_{\Gamma_i}$. The two latter data together with the known elements defining F_ϵ^* are used to compute the following relative errors :

$$\begin{aligned} err_D &= \frac{\|\tau_N - u|_{\Gamma_i}\|_{0, \Gamma_i}}{\|u|_{\Gamma_i}\|_{0, \Gamma_i}}, & err_N &= \frac{\|\eta_N - \sigma(u, p)n|_{\Gamma_i}\|_{0, \Gamma_i}}{\|\sigma(u, p)n|_{\Gamma_i}\|_{0, \Gamma_i}}, \\ err_P &= \frac{\|P_{ex} - P_{op}\|_2}{\|P_{ex}\|_2}, & err_\lambda &= \frac{\|\Lambda_{ex} - \Lambda_{op}\|_2}{\|\Lambda_{ex}\|_2}, \end{aligned} \quad (30)$$

where $(\eta_N, \tau_N; \phi_N)$ is the approximate Nash equilibrium output from Algorithm 1, and $\|\cdot\|_2$ represents the Euclidean norm. These metrics are used to assess the efficiency of our approach. The stability w.r.t. noise was stressed by solving the coupled problem with noisy perturbations of the Dirichlet data $G^\sigma = G(1 + \sigma\delta)$, with δ is a random real number taken from the uniform distribution over the interval $[-1, 1]$.

An arbitrary initial guess such as $S^{(0)} = (\eta^{(0)}, \tau^{(0)}, \lambda^{(0)}) = (0, 0, 0.1)$ and $F_\epsilon = 0$ are chosen to start the algorithm, and the relaxation parameter α is set to 0.25. The pointwise forces identified are represented in the domain Ω as a disc of radius $\epsilon = 0.07$.

The solvers for Stokes, the computation of the topological gradient and adjoint systems, and the minimization algorithms as well, were implemented using the Finite Element package FreeFem++ [18].

Example 1: An annular domain.

We consider an annular domain Ω with circular boundary components Γ_i and Γ_c , both centered at $(0, 0)$ and with radii $R_i = 1$ and $R_c = 2$, respectively. In this example, we choose $(\beta, \gamma) = (0, 1)$, and the Cauchy data $\sigma(u, p)n|_{\Gamma_c}$ is generated via the solution of the problem (4), with $G|_{\Gamma_c} = (y^2, x^2)$ and $\Psi|_{\Gamma_i} = -(x, y)$.

Test-case A.

The exact source-term is located at $P_{ex} = (1.8, 0)$, with an intensity source $\Lambda_{ex} = (0.2, 0.2)$.

We applied our algorithm 1, presented in section 3, to compute the Nash equilibrium. Figure 5 presents the obtained results. We remark that these results are in good accordance with the exact source F_ϵ and missing data.

For the case of noisy Dirichlet data G^σ given over Γ_c , it can be seen from the profiles presented in Figure 6 and the Table 4 that the boundary data recovery is overall stable with respect to the noise magnitude, in particular the computed components of the normal stress are more sensitive than the velocity one, and the estimated elements defining F_ϵ , identified source and their intensity forces, are also acceptable.

The relative errors defined by formulas (30) are summarized in Table 1 for the test-case A.

Table 1: Test-case A. L^2 relative errors on missing data on Γ_i (on Dirichlet and Neumann data), and the relative errors on the identified source position and on the identified source intensity for various noise levels.

Noise level	err_D	err_N	err_P	err_Λ
$\sigma = 0\%$	0.003	0.060	0.010	0.018
$\sigma = 1\%$	0.008	0.087	0.010	0.155
$\sigma = 3\%$	0.015	0.147	0.043	0.169

1 *Test-case B. The case of multiple points-forces.*

2
3 In this test-case, we try to detect and locate multiple point-forces. We propose to identify four pointwise
4 forces, located respective at the points $P_1 = (1.8, 0)$, $P_2 = (0, 1.8)$, $P_3 = (-1.8, 0)$ and $P_4 = (0, -1.8)$, and
5 their exact intensity force λ_i is equal to $(0.2, 0.2)$, $i=1, \dots, 4$.

6
7 We suppose that the number m of the region $\mathcal{S}_{P_i, \epsilon}$, $i=1, \dots, m$, is unknown. We observe from Figure 7(a)(b)
8 that our proposed algorithm is able to determine the number of the small region inside Ω and gives a good
9 approximation of the locations and the recovery intensity for each components of the source-term, as well
10 as the recovered data Figure 7(c)-(f). The recovery of missing boundary data and the estimated value of P
11 and λ are stable with respect to noisy Dirichlet measurements, as shown Figure 8 and Table 5, where the
12 table 5 presents the different error at convergence.

13 To assess our algorithm and results against the so-called inverse crime, that possibly arises when the
14 same model is used to synthesize Cauchy data and to solve the corresponding inverse problem, resulting in
15 possible artificial outperformance, we synthesized Cauchy data using different meshes, see Figure 2. All our
16 numerical experiments produced results of the same good quality than the results presented in Figure 7, see
17 Figure 9.

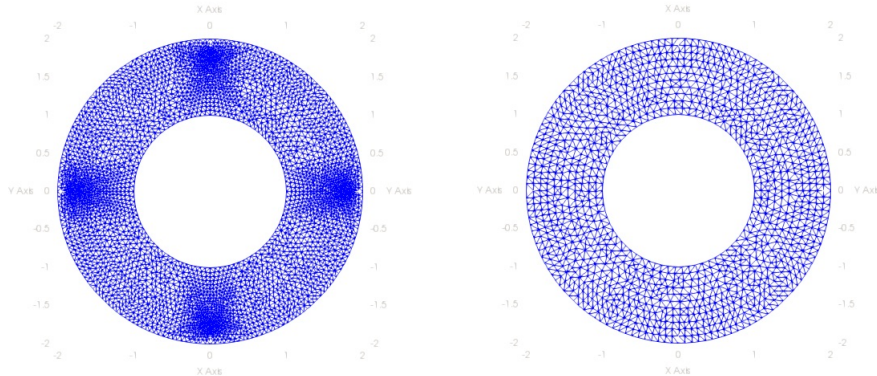


Figure 2: Test case B. (Left) Mesh used for solving the direct problem, in order to construct the synthetic data. (Right) Mesh used for solving the coupled inverse problem, with P2-P1 finite element.

18 *Example 2: A geometry with corners.*

19 The domain is a centered square $] -0.5, 0.5[\times] -0.5, 0.5[$, the finite element discretization of the domain
20 boundary $\partial\Omega$ is constituted of 160 vertices. We impose here $(\beta, \gamma) = (1, 0)$, and $G = H = (2y^2 - 1/2, 0)$
21 prescribed over $\partial\Omega$.

22 Overspecified Cauchy data are prescribed on the boundaries $y \in \{-\frac{1}{2}, \frac{1}{2}\}$ and $x = -1/2$ of the square and
23 the underspecified boundary data $u|_{\Gamma_i} = u(1/2, y)$ and its stress force are sought.

1 *Test-case C.*

2 The exact source-term is located at $P_{ex} = (-0.3, -0.25)$, with intensity $\Lambda_{ex} = (0.25, 0.2)$.

3
4 The numerically obtained results are shown in Figure 10. Figure 10(a) presents the iso-values of the
5 topological gradient, the source support $\mathcal{S}_{x_0, \epsilon}$ can be located in the areas where the topological gradient is
6 negative. The estimated intensity and the determined position are very satisfactory, as shown Figure 10(b).
7 The numerical Dirichlet solution is a good approximation for the exact solution one, see Figure 10(c)(d).
8 Then, concerning the numerical Neumann solution, see Figure 10(e)(f), it can be seen that the estimates
9 deviate from the exact one, especially near the endpoints of the boundary which is the region of singularities,
10 in the corners. There is also a remarkable stability with respect to noisy data of both the estimated elements
11 and the recovered boundary data, see Figure 11 and Table 6.

12 The relative errors presented in Table 2 show the performance of our method with respect to noisy
13 Dirichlet measurements.

Table 2: Test-case C. L^2 relative errors on missing data on Γ_i (on Dirichlet and Neumann data), and the relative errors on the identified source position and on the identified source intensity for various noise levels.

Noise level	err_D	err_N	err_P	err_Λ
$\sigma = 0\%$	0.011	0.097	0.071	0.009
$\sigma = 1\%$	0.011	0.102	0.136	0.029
$\sigma = 3\%$	0.021	0.106	0.184	0.058

14 A numerical study concerning the sensitivity of the reconstruction according to the position of the source
15 term in the domain has been studied. The Figure 3 shows that the relative errors increase when the source
16 term becomes closer to the inaccessible boundary Γ_i .

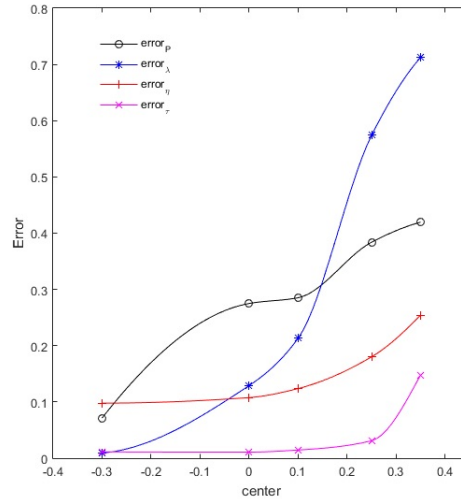


Figure 3: Test case C. Sensitivity of the reconstruction w.r.t. the distance to the inaccessible boundary Γ_i , the distance of the center of $\mathcal{S}_{P, \epsilon}$ from Γ_i , for $y = -0.25$.

17 *The 3D case.*

18 We present hereafter an example of numerical reconstruction in the three dimensional case. The domain
19 Ω is a cube $(0, 1)^3$, such that its boundary splitted into two parts Γ_i and Γ_c , where $\Gamma_i = \{(x, y, z) \in$

20 $\partial\Omega$; such that $x = 1$ represents the inaccessible part and $\Gamma_c = \partial\Omega \setminus \Gamma_i$ is the accessible part, where the
 21 Cauchy data is available. We try so to detect a source F_ϵ located in $P_{ex} = (0.25, 0.25, 0.25)$ and with a source
 1 intensity $\lambda_{ex} = (0.25, 0.2, 0)$. The Cauchy data on Γ_c are numerically simulated by solving the following
 2 Dirichlet problem:

$$\begin{cases} -\operatorname{div}(\sigma(u, p)) = F_\epsilon^* & \text{in } \Omega, \\ \operatorname{div} u = 0 & \text{in } \Omega, \\ u = G & \text{on } \partial\Omega, \end{cases}$$

3 where G is a given function. Then, applying our algorithm 1 in order to find the Nash equilibrium, which
 4 is expected to approximate the coupled problem solution. The finite element computations are performed
 5 with 4,096 nodes and 20,250 tetrahedral elements. The cost of computation is quite expensive, to overcome
 6 this difficulty, we use `ffdm` which implements a class of parallel solvers in `FreeFem`. The obtained results
 7 are presented in Table 3, with noise free Dirichlet data over Γ_c . The Figure 4 represents the iso-values of the
 8 topological gradient at convergence.

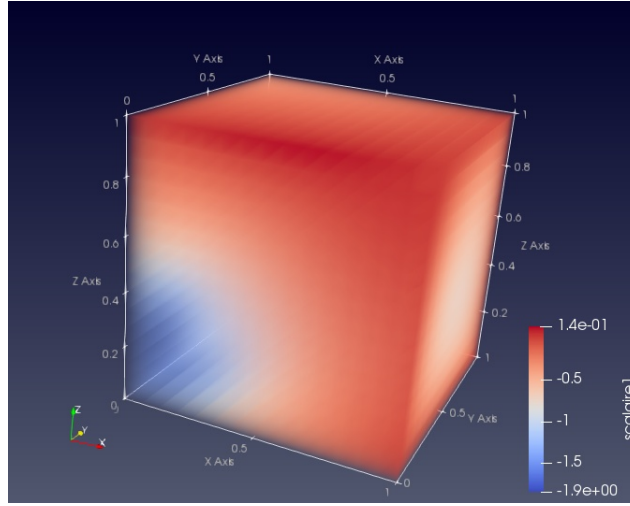


Figure 4: The iso-values of the topological gradient at convergence, $P_{op} = (0.2, 0.2, 0.2)$ and $\Lambda_{op} = (0.233, 0.204, 0.005)$. Exact values: $P_{ex} = (0.25, 0.25, 0.25)$ and $\Lambda_{ex} = (0.25, 0.2, 0)$.

Table 3: L^2 relative errors of reconstructed solution in the whole domain and missing data on Γ_i (on Dirichlet and Neumann data), and the relative errors on the identified source position and on the identified source intensity for noise-free, where $err_{u_i} = \|u_{i,\epsilon} - u\|_{0,\Omega} / \|u\|_{0,\Omega}$, for $i = 1, 2$.

err_{u_1}	err_{u_2}	err_τ	err_η	err_P	err_Λ
0.008	0.026	0.031	0.224	0.2	0.056

9 5. Conclusion

10 we have addressed, in the present paper, the problem of identifying the location and magnitude of a finite
 11 but unknown number of point-wise sources, in a linear steady Stokes problem with missing boundary data.
 12 Such a reconstruction problem couples two inverse problems of different classes, the recovery of missing
 13 boundary data (the Cauchy problem), and the identification of point-wise sources. Each of these two
 14 inverse problems is known to be severely ill-posed by its own, and designing efficient and stable algorithms

15 is challenging. In our case, the problem of designing efficient and robust algorithms is worsened by the
1 coupling of the two ill-posed problems, and by the fact that we consider as available only a single pair of
2 over-specified data (and not the classical Dirichlet-to-Neumann whole map).

3 Due to the identification/recovery coupling, classical methods fail, mainly because of being too specific
4 to each of the source identification or data recovery problems. Hence our recourse to game theory, which
5 is, by its very nature, able to address such antagonistic situations. Previous successful reframing of data
6 recovery inverse problems as Nash games has fostered the formulation of the coupled source identification
7 and data recovery problems as Nash games.

8 We have proposed here to formulate the coupled inverse problems as a static with complete information
9 Nash game. First, we have relaxed the point-wise source identification problem to gain some regularity on
10 the velocity and pressure state variables, and we have introduced three players and three cost functionals.
11 The two first, named Dirichlet-Neumann players, were dedicated to ensure the data completion while the
12 third one was dedicated to ensure the detection of the sources. We postulated that the sought solution of
13 the coupled problem could be found as a Nash equilibrium of the three-player game.

14 This formulation resulted in the design of a novel algorithm, which is composed of two main steps. In
15 the first step, the third player seeks to identify the number and location of the sources using a topological
16 gradient method. In the second one, the two Dirichlet-Neumann players solve the data completion, in a
17 parallel task with the third player, which minimizes a Kohn-Vogelius like functional in order to identify the
18 different sources magnitudes.

19 The efficiency and robustness of our coupled reconstruction algorithm was proved against several numer-
20 ical experiments led for different two- and three-dimensional test-cases.

21 *Acknowledgments.* This work was financially supported by the PHC Utique program NAMRED of the
22 French Ministry of Foreign Affairs and Ministry of higher education, research and innovation and the Tunisian
23 Ministry of higher education and scientific research in the CMCU project number 18G1502.

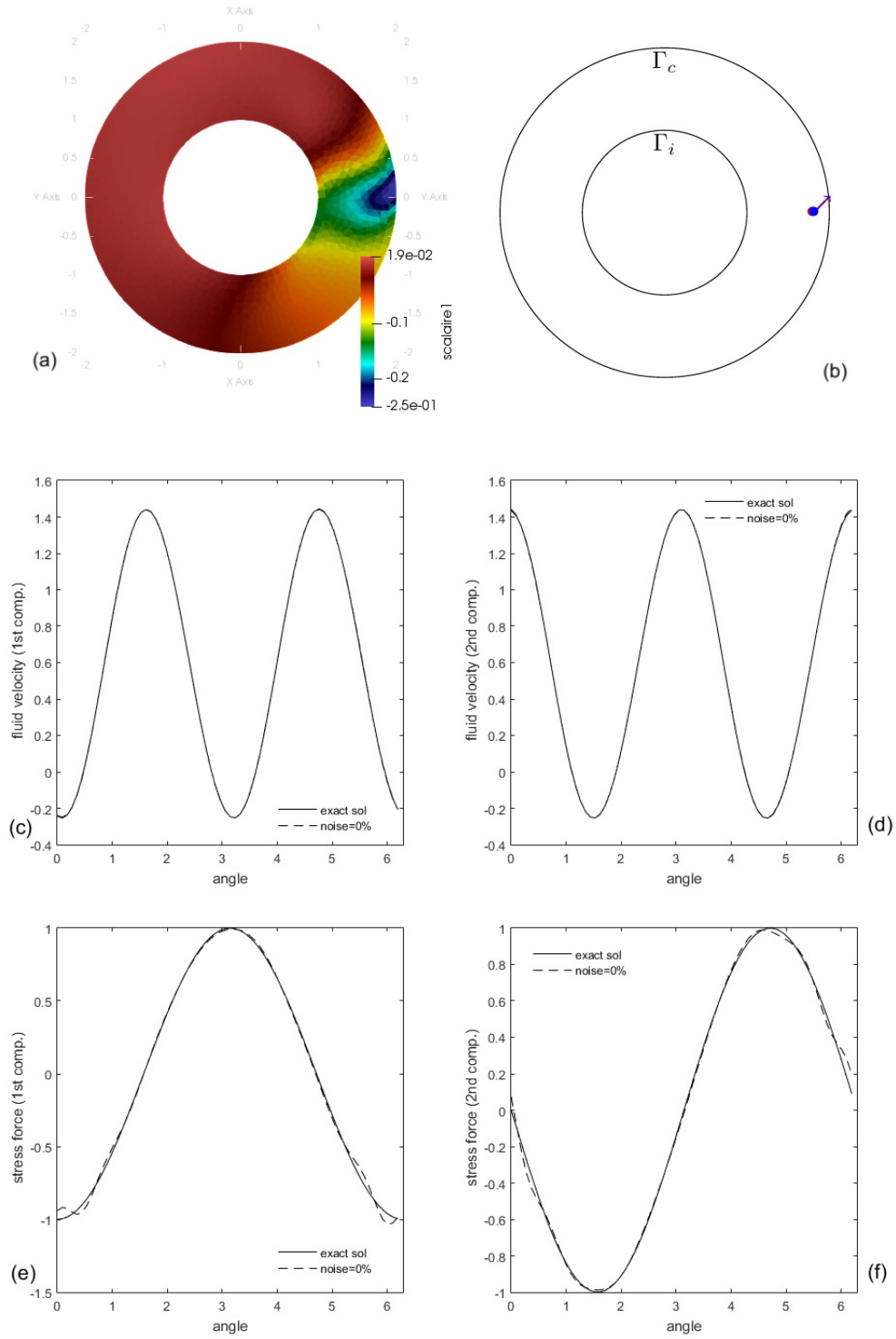


Figure 5: Test case A. Reconstruction of the point-forces and missing boundary data with noise free Dirichlet data over Γ_c . (a) the iso-values of the topological gradient at convergence. (b) exact elements defining the source-term -red vector- and computed one -blue vector- (c) exact -line- and computed -dashed line- first component of the velocity over Γ_i . (d) exact -line- and computed -dashed line- second component of the velocity over Γ_i . (e) exact -line- and computed -dashed line- first component of the normal stress over Γ_i (f) exact -line- and computed -dashed line- second component of the normal stress over Γ_i .

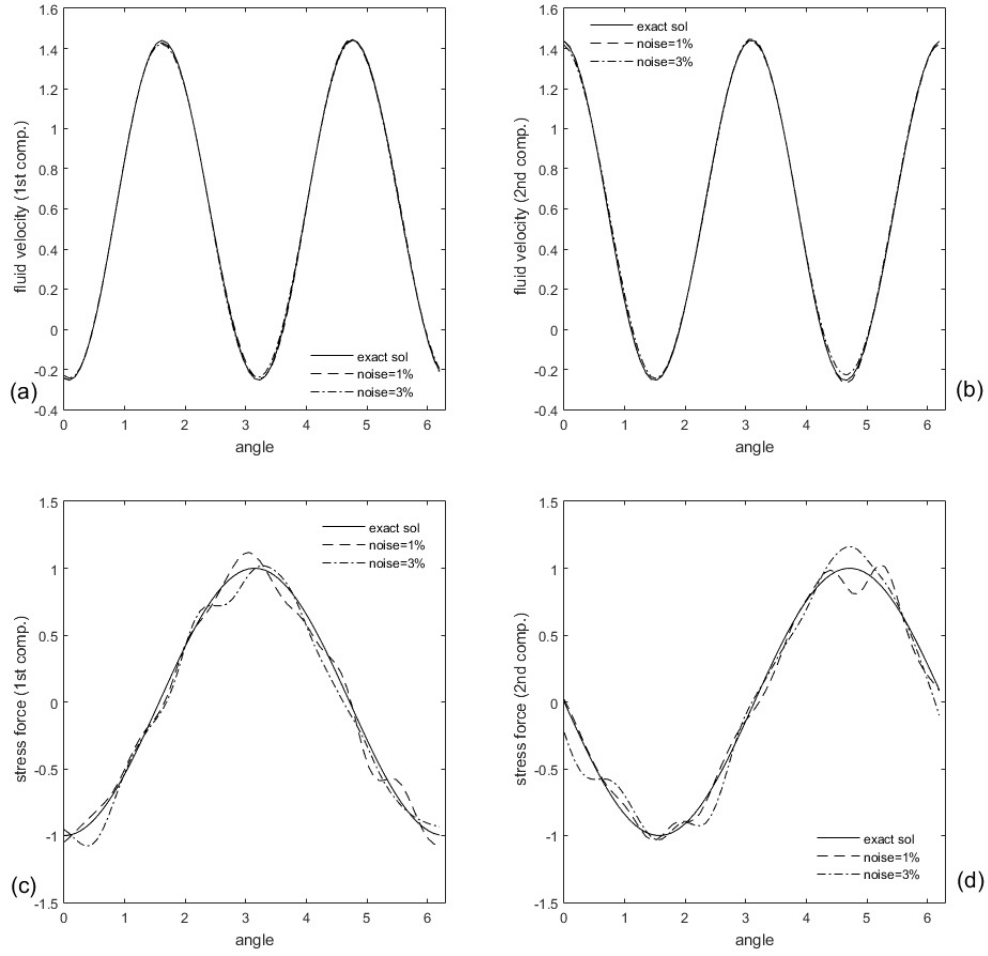


Figure 6: Test case A. Reconstruction of the missing boundary data with noisy Dirichlet data over Γ_c with noise levels $\sigma = \{1\%, 3\%\}$. **(a)** exact and computed first components of the velocity over Γ_i **(b)** exact and computed second components of the velocity over Γ_i **(c)** exact and computed first components of the normal stress over Γ_i **(d)** exact and computed second components of the normal stress over Γ_i .

Table 4: Test-case A. Identified source position and their intensity for various noise levels.

Noise level	$\sigma = 0\%$	$\sigma = 1\%$	$\sigma = 3\%$	
P_{op}	(1.81,-2e-09)	(1.81,-2.e-09)	(1.84,-0.066)	$P_{ex} = (1.8, 0)$
Λ_{op}	(0.195,0.202)	(0.161,0.179)	(0.2,0.152)	$\Lambda_{ex} = (0.2, 0.2)$

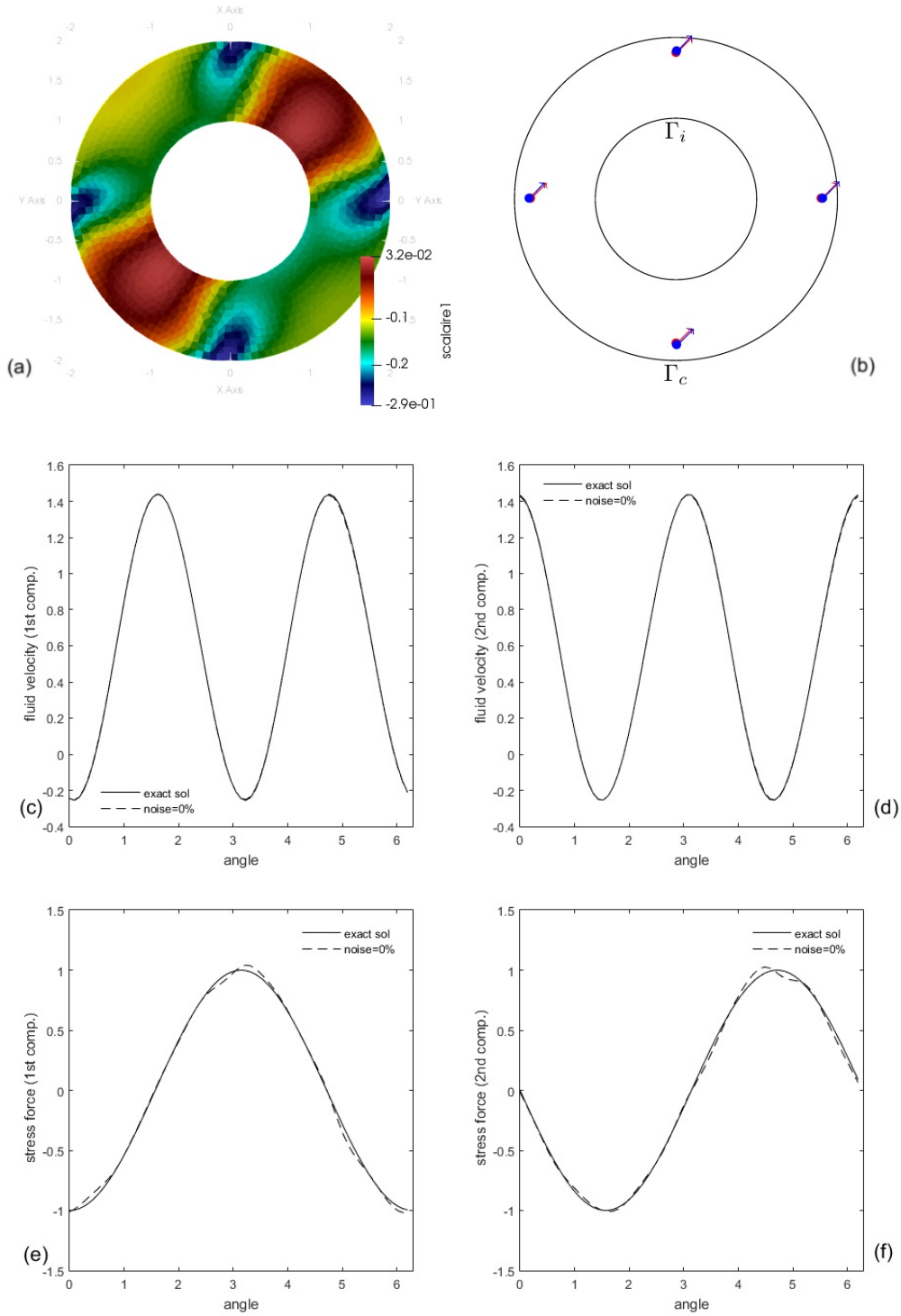


Figure 7: Test case B. Reconstruction of the point-forces and missing boundary data with noise free Dirichlet data over Γ_c . (a) the iso-values of the topological gradient at convergence. (b) exact elements defining the source-term -red vector- and computed one -blue vector- (c) exact -line- and computed -dashed line- first component of the velocity over Γ_i . (d) exact -line- and computed -dashed line- second component of the velocity over Γ_i . (e) exact -line- and computed -dashed line- first component of the normal stress over Γ_i . (f) exact -line- and computed -dashed line- second component of the normal stress over Γ_i .

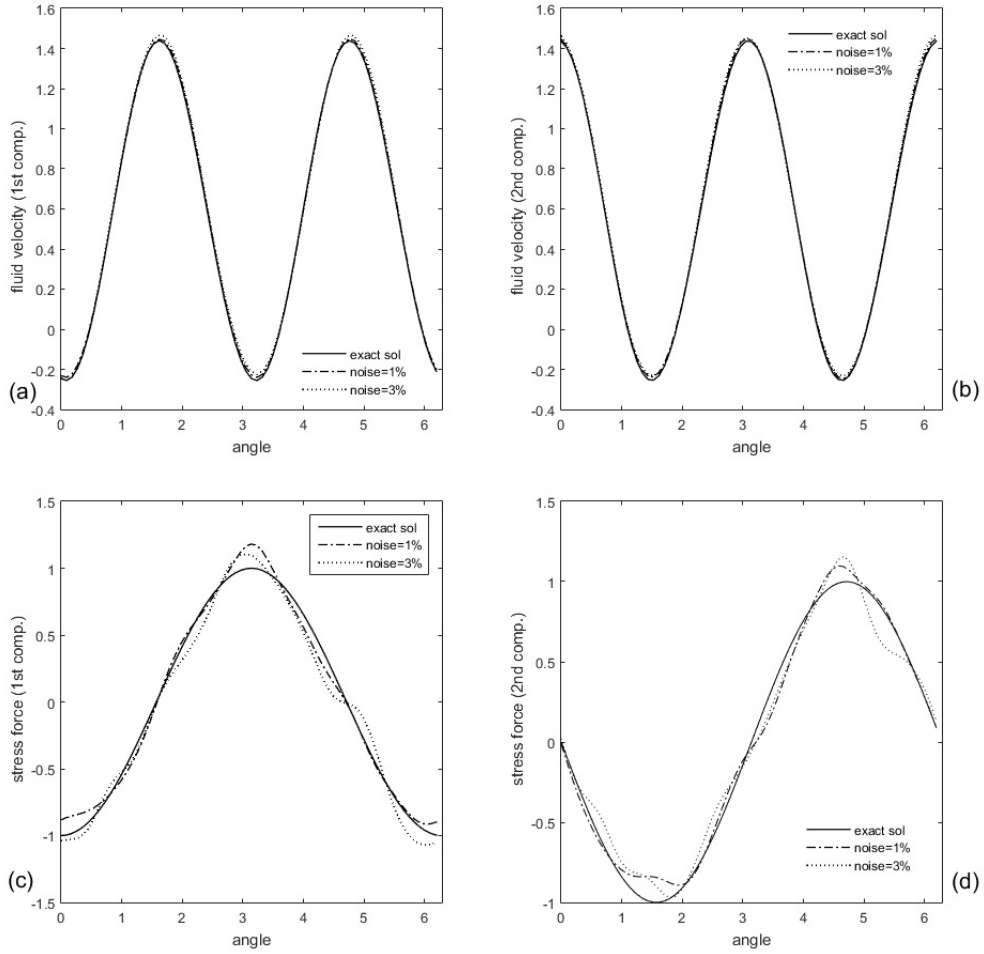


Figure 8: Test case B. Reconstruction of the missing boundary data with noisy Dirichlet data over Γ_c with noise levels $\sigma = \{1\%, 3\%\}$. (a) exact and computed first components of the velocity over Γ_i (b) exact and computed second components of the velocity over Γ_i (c) exact and computed first components of the normal stress over Γ_i (d) exact and computed second components of the normal stress over Γ_i .

Table 5: Test-case B. L^2 relative errors on missing data on Γ_i (on Dirichlet and Neumann data), and the relative errors on the identified source position and on the identified source intensity for various noise levels.

Noise level	err_D	err_N	err_P	err_Λ
$\sigma = 0\%$	0.005	0.056	0.010	0.049
$\sigma = 1\%$	0.013	0.113	0.010	0.181
$\sigma = 3\%$	0.025	0.141	0.043	0.24

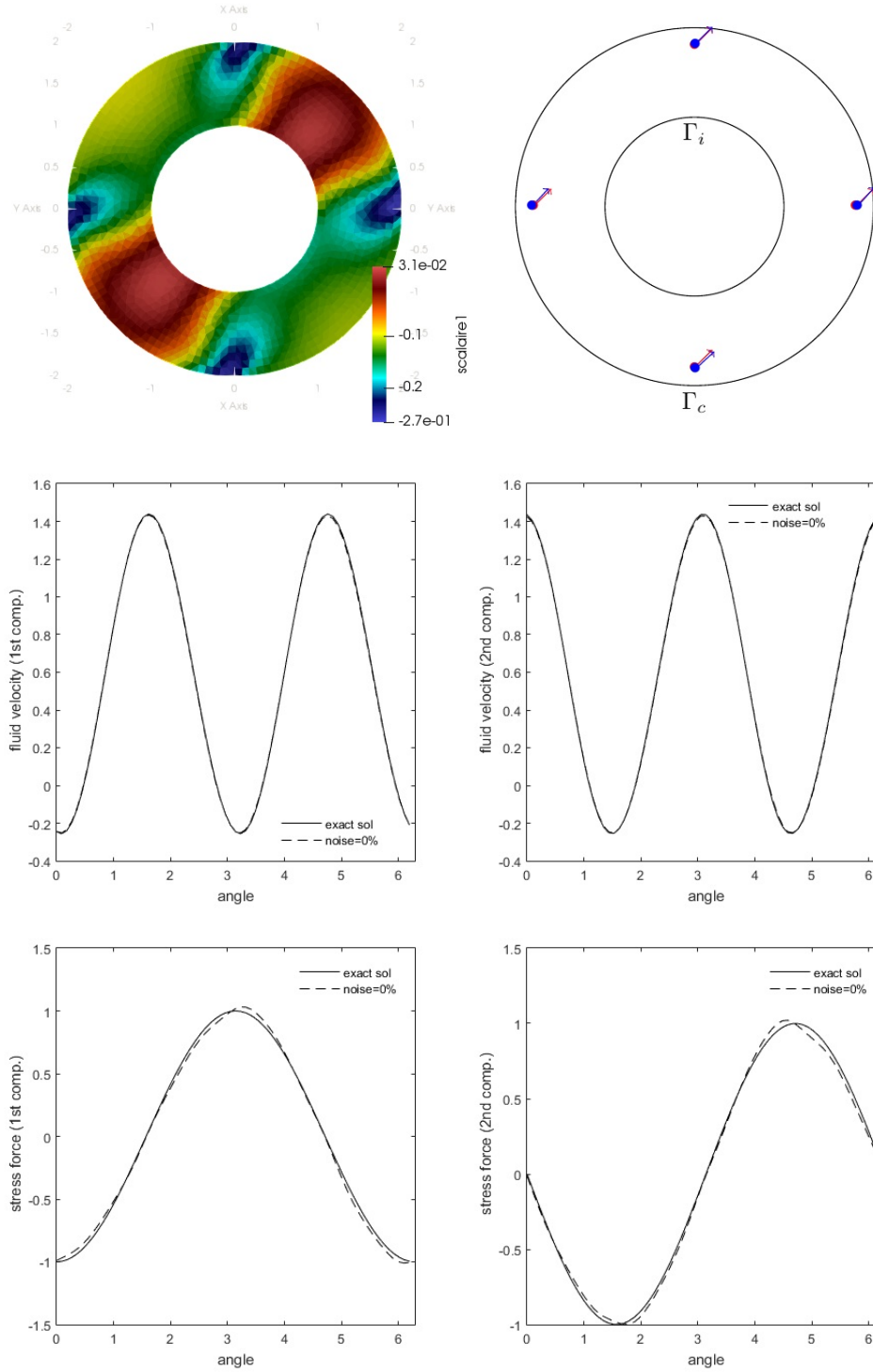


Figure 9: Test case B: Assessing Inverse-Crime-Free reconstruction. Test case B. Top: the iso-values of the topological gradient at convergence, and the exact and optimal elements defining the source-term. Middle: the two components of the velocity on Γ_i . Bottom: the two components of the normal stress on Γ_i ($err_\tau = 0.00768152$, $err_\eta = 0.0713575$, $err_P = 0.0105486$, and $err_\Lambda = 0.0560551$).

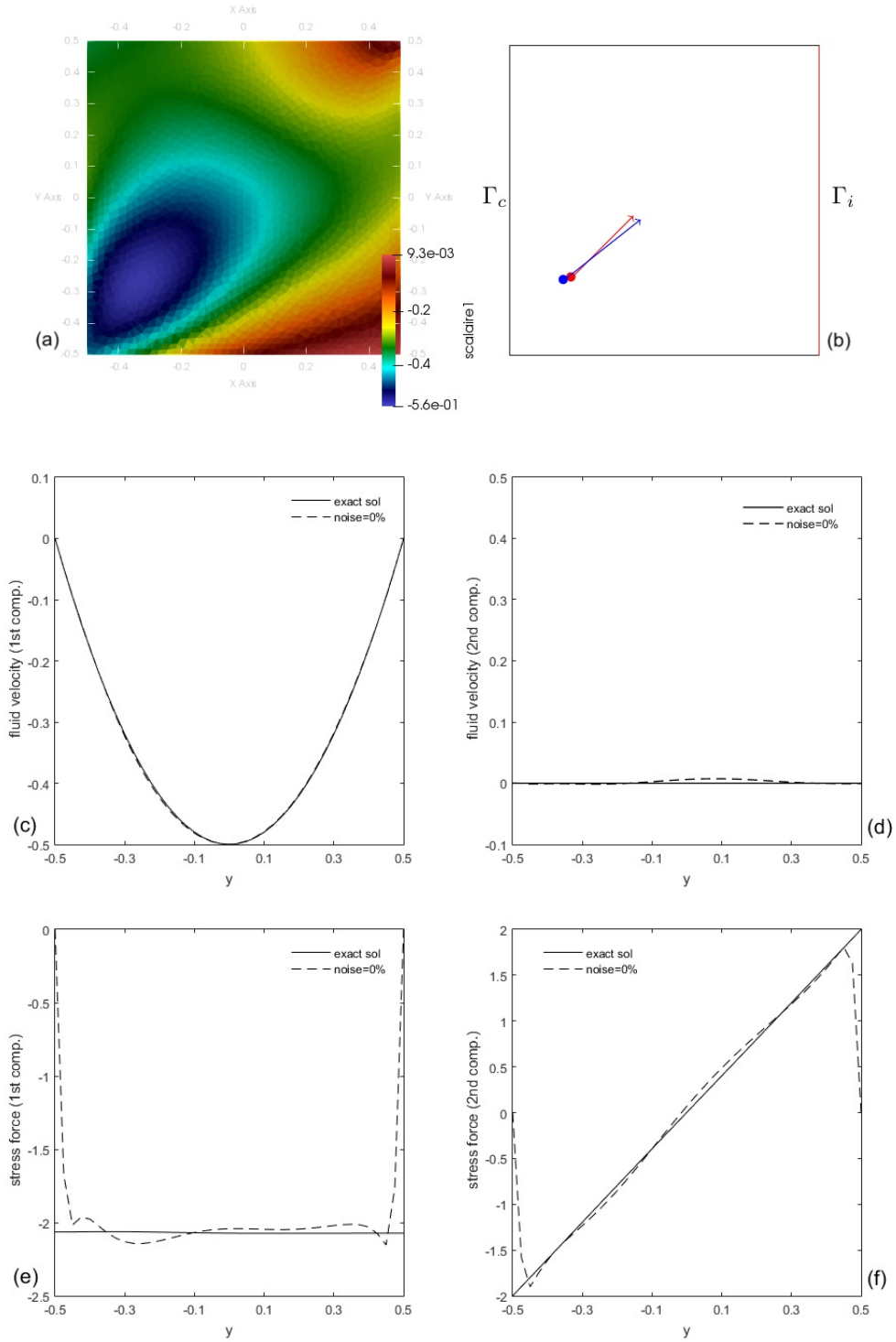


Figure 10: Test case C. Reconstruction of the point-forces and missing boundary data with noise free Dirichlet data over Γ_c . (a) the iso-values of the topological gradient at convergence. (b) exact elements defining the source-term -red vector- and computed one -blue vector- (c) exact -line- and computed -dashed line- first component of the velocity over Γ_i . (d) exact -line- and computed -dashed line- second component of the velocity over Γ_i . (e) exact -line- and computed -dashed line- first component of the normal stress over Γ_i (f) exact -line- and computed -dashed line- second component of the normal stress over Γ_i .

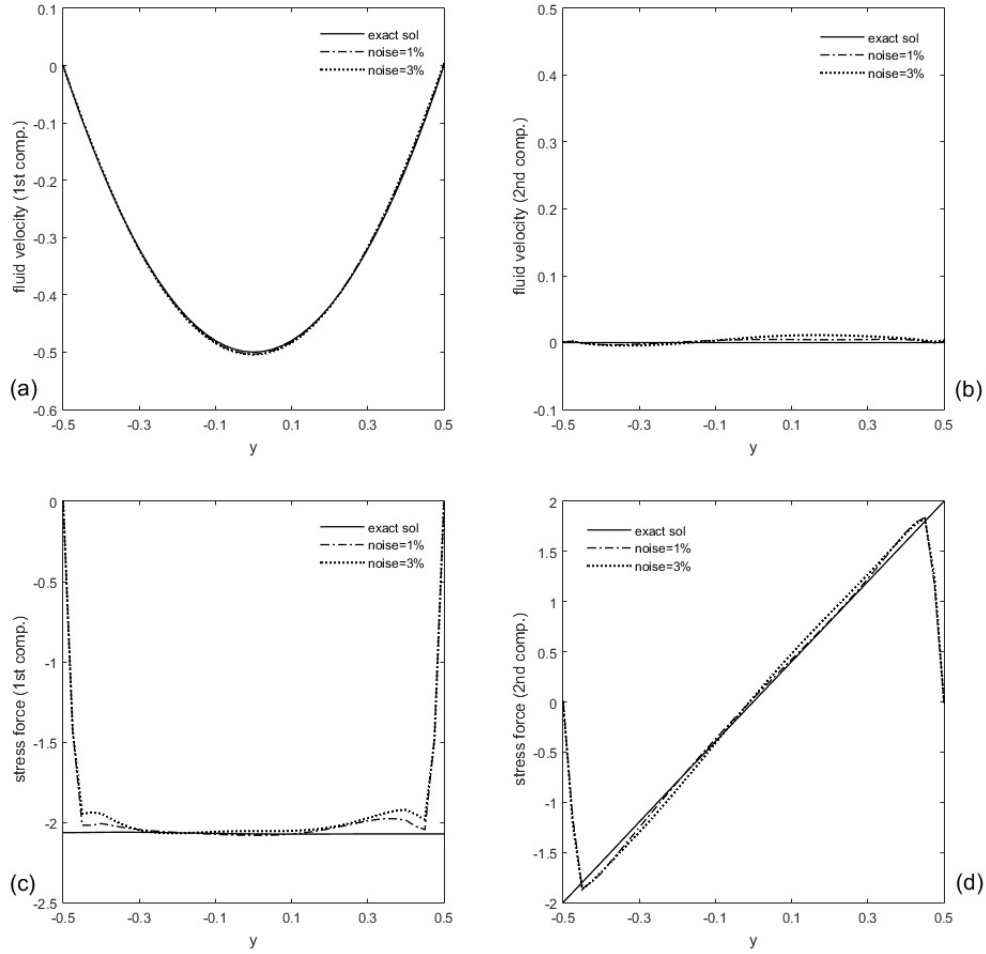


Figure 11: Test case C. Reconstruction of the missing boundary data with noisy Dirichlet data over Γ_c with noise levels $\sigma = \{1\%, 3\%\}$. (a) exact and computed first components of the velocity over Γ_i (b) exact and computed second components of the velocity over Γ_i (c) exact and computed first components of the normal stress over Γ_i (d) exact and computed second components of the normal stress over Γ_i .

Table 6: Test-case C. Identified source position and their intensity for various noise levels.

Noise level	$\sigma = 0\%$	$\sigma = 1\%$	$\sigma = 3\%$	
P_{op}	(-0.326,-0.259)	(-0.339,-0.285)	(-0.36,-0.29)	$P_{ex} = (-0.3, -0.25)$
Λ_{op}	(0.248,0.197)	(0.24,0.199)	(0.231, 0.196)	$\Lambda_{ex} = (0.25, 0.2)$

1 References

- 2 [1] R. Aboulaich, A. Ben Abda, and M. Kallel. A control type method for solving the Cauchy-Stokes problem. *Applied*
- 3 *Mathematical Modelling*, 37:4295–4304, 2013.
- 4 [2] C. J. S. Alves and A. L. Silvestre. On the determination of point-forces on a Stokes system. *Mathematics and Computers*
- 5 *in Simulation*, 66:385–397, 2004.
- 6 [3] G. Bastay, T. Johansson, V. A. Kozlov, and D. Lesnic. An alternating method for the stationary Stokes system. *Z. Angew.*
- 7 *Math. Mech*, 86:268–280, 2006.

- 1 [4] L. Bourgeois. A mixed formulation of quasi-reversibility to solve the Cauchy problem for Laplace's equation. *Inverse*
2 *Problems*, 21:1087–1104, 2005.
- 3 [5] F. Caubet. *Détection d'un Objet Immergé dans un Fluide*. PhD thesis, Université de Pau, 2012.
- 4 [6] R. Chamekh, A. Habbal, M. Kallel, and N. Zemzemi. A Nash game algorithm for the solution of coupled conductivity
5 identification and data completion in cardiac electrophysiology. *Mathematical Modelling of Natural Phenomena*, 14:Art.
6 201, 15 pp, 2019.
- 7 [7] A. Cimetière, F. Delvare, and F. Pons. Solution of the Cauchy problem using iterated tikhonov regularization. *Inverse*
8 *Problems*, 17:553–570, 2001.
- 9 [8] P. Constantin and C. Foias. *Navier-Stokes Equations*. University of Chicago Press, 1988.
- 10 [9] A. El Badia and T. Ha-Duong. An inverse source problem in potential analysis. *Inverse Problem*, 16:651–663, 2000.
- 11 [10] H.A. Eschenauer, V. Kobelev, and A. Schumacher. Bubble method for topology and shape optimization of structures.
12 *Structural Optimization*, 8:42–51, 1994.
- 13 [11] C. Fabre and G. Lebeau. Unique continuation property of solutions of the stokes equation. *Communications in Partial*
14 *Differential Equations*, 21:573–596, 1996.
- 15 [12] R.S. Falk and P.B. Monk. Logarithmic convexity for discrete harmonic functions and the approximation of the Cauchy
16 problem for poisson's equation. *Mathematics of Computation*, 47:135–149, 1986.
- 17 [13] J. Ferchichi, M. Hassine, and H. Khenous. Detection of point-forces location using topological algorithm in Stokes flows.
18 *Applied Mathematics and Computation*, 12:7056–7074, 2013.
- 19 [14] P. C. Franzone and E. Mageses. On the inverse potential problem of electrocardiology. *Calcolo*, 16:459–538, 1979.
- 20 [15] A. Habbal and M. Kallel. Neumann-Dirichlet Nash strategies for the solution of elliptic Cauchy problems. *SIAM Journal*
21 *on Control and Optimization*, 51:4066–4083, 2013.
- 22 [16] A. Habbal, M. Kallel, and M. Ouni. Nash strategies for the inverse inclusion Cauchy-Stokes problem. *Inverse problems*
23 *and imaging*, 13:827–862, 2019.
- 24 [17] J. Hadamard. *The Cauchy Problem and the Linear Hyperbolic Partial Differential Equations*. Dover, New York, 1953.
- 25 [18] F. Hecht. New development in freefem++. *Journal of Numerical Mathematics*, 20:251–265, 2012.
- 26 [19] T. Johansson and D. Lesnic. Reconstruction of a stationary flow from incomplete boundary data using iterative methods.
27 *European Journal of Applied Mathematics*, 17:651–663, 2006.
- 28 [20] V. Kozlov, V. Maz'ya, and A. Fomin. An iterative method for solving the Cauchy problems for elliptic equations.
29 *Computational Mathematics and Mathematical Physics*, 31:45–52, 1991.
- 30 [21] W. Mansouri, T. N. Baranger, H. Ben Ameer, and N. H. Tlatli. Identification of injection and extraction wells from
31 overspecified boundary data. *Inverse Problems in Science and Engineering*, 25:1091–1111, 2017.
- 32 [22] A. Samuel, I. Horchani, and M. Masmoudi. Crack detection by the topological gradient method. *Control and cybernetics*,
33 34:81–101, 2005.
- 34 [23] J. Sokolowski and A. Zochowski. On the topological derivative in shape optimization. *SIAM Journal on Control and*
35 *Optimization*, 37:1251–1272, 1999.
- 36 [24] A. Stephane, A. Ben Abda, and T.N. Baranger. Solving Cauchy problems by minimizing an energy-like functional. *Inverse*
37 *problems*, 22:115–133, 2006.
- 38 [25] R. Temam. *Navier-Stokes Equations: Theory and Numerical Analysis*. American Mathematical Society, 2001.